University of Pisa

Department of Information Engineering

Master's Thesis in
Telecommunication Engineering

Power allocation algorithms in point-to-point and interference channels for BIC-OFDM systems

Author:
Elia Guidi

Supervisors:
Prof. Filippo Giannetti
Ing. Vincenzo Lottici
Ing. Riccardo Andreotti

July 25^{th}, 2014

Contents

List of Acronyms

AMC	*Adaptive Modulation and Coding*
AWGN	*Additive With Gaussian Noise*
ARQ	*Automatic Repeat Request*
BER	*Bit Error Rate*
BIC	*Bit Interleaving Coding*
CBS	*Coded Binary Symbols*
CC	*Convolutional Code*
CRC	*Cyclic Redundancy Check*
CSI	*Channel State Information*
EGP	*Expected GoodPut*
ESM	*Effective SNR Mapping*
FER	*Frame Error Rate*
FFT	*Fast Fourier Transformer*
GP	*GoodPut*
IFFT	*Inverse Fast Fourier Transformer*
LLR	*Log-Likelihood Ratio*
LRA	*Link Resource Adaptation*
LTE	*Long Term Evolution*
PA	*Power Allocated*
SBS	*Small Base Station*

GPR	*Goodput to power ratio*
MUI	*Multiple User Interference*
MGF	*Moment Generating Function*
MIMO	*Multiple Input Multiple Output*
ML	*Maximum Likelihood*
MB	*Multiple Beamforming*
NOAS	*Number of Active Subcarries*
OFDM	*Orthogonal Frequency Division Multiplexing*
PA	*Power Allocation*
PDU	*Physical Data Unit*
PEP	*Packet Error Probability*
PER	*Packet Error Rate*
PHY	*Physical*
PU	*Primary User*
PDF	*Probability Density Function*
PSD	*Power Spectral Density*
PSR	*Packet Success Rate*
QAM	*Quadrature Amplitude Modulation*
QoS	*Quality of Service*
RLC	*Radio Link Control*
RV	*Random Variable*
RX	*Receiver*
SISO	*Single Input Single Output*
SNR	*Signal to Noise Ratio*
SU	*Secondary User*
SVD	*Singular Value Decomposition*
SW	*Soft Ware*
TM	*Transmit Modulation*
TX	*Transmitter*
TAP	*Total Allocated Power*
UBA	*Uniform Bit Allocation*
UPA	*Uniform Power Allocation*

Chapter 1

Introduction

Orthogonal frequency division multiplexing (OFDM) technology, in combination with advanced features such as bit-interleaved coded modulation (BICM) [25] and link resource adaptation (LRA) [26] and resource allocation techniques (RA), have been identified as the building blocks for future wireless communication systems, in that they can meet the strict quality of service (i.e. high data rate, reliable communications) requirements of the users in the harsh propagation environment of the wireless multipath channel. Due to the proliferation of advanced mobile devices (i.e., smartphones, tablets), a 20-fold increase in data traffic is expected over the next few years, compelling mobile operators to find new ways to significantly boost their network capacity, provide better coverage, and reduce network congestion. In this context, the idea of heterogeneous networks (HetNets), consisting of a mix of short-range and low-cost small cell base stations (SBSs) underlaying the existing macrocellular network, has recently emerged as a key solution for solving this capacity crunch problem. The surest way to increase the system capacity of a wireless link is by getting the transmitter and receiver closer to each other, which creates the dual benefits of higher-quality links and more spatial reuse.

In a network with nomadic users, this inevitably involves deploying more infrastructure, typically in the form of microcells, hot spots, distributed antennas, or relays. The enormous gains reaped from smaller cell sizes arise from efficient spatial reuse of spectrum or, alternatively, higher area spectral efficiency and also from mitigate fading and reduce time dispersion on urban mobile radio channels. A microcell is a region served by radio base unit, just as in current cellular systems, only smaller in area by one-to-two orders of magnitude. Traditional cells, called *macrocells*, are served using costly base stations with antenna towers 50 m high or more, and are limited by zoning, economics, and other factors to radii no smaller than about 1 km. *Microcells*, on the other hand, would be served by compact, low-cost base units mounted on a lampposts or utility poles, at heights of about 10 m, and would have radii of 150 m or even less. They could be used to reach "dead spots" caused in traditional cellular areas by shadowing, or they could be used to serve subscribers on foot carrying low-power portables with small antennas. They could also exist indoors, for example, in malls, airports, train station, hotels, and office buildings.

On the other side the next generation wireless networks are expected to provide high speed internet access anywhere and anytime. The popularity of iPhone and other types of smartphones doubtlessly accelerates the process and creates new traffic demand, such as mobile video and gaming. The exponentially growing data traffic and the requirement of ubiquitous access have triggered dramatic expansion of network infrastructures and fast escalation of energy demand, which directly results in the increase of greenhouse gas emission and becomes a major threat for environmental protection and sustainable development. To meet the challenges raised by the high demand of wireless traffic and energy consumption, green evolution has become an urgent need for wireless net-

works today. Therefore, increasing the energy efficiency of radio networks as a whole can be an effective approach. Reducing the energy consumption is not only a matter of being environment-aware, it is also very much an economically important issue, especially from the standpoint of operators. Vodafone, for example, has foreseen energy efficiency improvement as one of the most important areas that demand innovation for wireless standards beyond LTE. Link adaptation based on channel state information (CSI) is normally used to maximize throughput for a given total transmit power. However, link adaptation can also be directed towards maximizing energy efficiency. In addition, energy efficiency is becoming increasingly important for mobile communications because of the slow progress of battery technology and growing requirements of anytime and anywhere multimedia applications. With sufficient battery power, link adaptation can be geared toward peak performance delivery. However, with limited battery capacity, link adaptation could be adapted toward energy conservation to minimize battery drain. Energy efficient communication also has the desirable benefit of reducing interference to other co-channel users as well as lessening environmental impacts, e.g. heat dissipation and electronic pollution. For energy-efficient communications we mean the number of bits that can be reliably conveyed over the channel per unit of energy consumed. So, improving the energy efficiency involves minimizing the energy consumption per bit [14] or equivalently maximizing the throughput per Joule metric [15]. Hence, more network capacity on the one hand, and less energy consumption on the other, are the seemingly contradictory future requirements on ICT. This has stimulated an intense research activity in both academia and industry in an innovative research area (recently spurred out by the SMART 2020 report [18] and the GreenTouch consortium [20]) called green cellular networks [19], whose ultimate goal is to design the architectures and technolo-

gies needed to meet the explosive growth in cellular data demand while reducing energy consumption.

In this thesis, we tackle the problem of concurrent communications of users in small cells environment based on packet-oriented BIC-OFDM signalling, competing against each other for the same bandwidth to minimize their total allocated power (TAP) under a constraint on the *Goodput* (GP). One of the most effective frameworks to theoretically model such a problem is the game theory. In particular, we will resort to noncooperative games, where the stable output, i.e., the Nash equilibrium, represents a feasible set of power allocation vectors that minimizes the TAP of each user. According to the game theory framework, the problem under study is described in strategic form wherein the set of players, utilities and strategies are represented by the competitive users, the ESNRs and the set of feasible power allocations, respectively. In particular, the set of feasible power allocation vectors have to satisfy a constraint on GP. A novel distributed algorithm based on the *best response* (BR) is proposed, which allows to evaluate an equilibrium solution and verify the algorithm convergence. Unfortunately, for such a scenario, the packet error rate (PER), from wich the GP depends, is not available in closed-form. However, a very efficient solution can be obtained by resorting to the effective signal-to-noise-ratio (SNR) mapping (ESM) technique. This method allows each user to evaluate a single scalar value, named *effective* SNR (ESNR), accounting for all the signal-to-noise-plus-interference-ratios (SNIRs) experienced over the active subcarriers, and to univocally map it into a PER value.

Chapter 2

BIC-OFDM Overview

In this chapter the block diagram of a SISO BIC-OFDM transmission is showed, together with the detailed description of the processing performed over the signals. In addition we will see the *Link Resource Adaptation* (LRA), which makes an optimal choice for every subcarrier about transmission power, modulation and code, according to channel conditions, present during the transmission of a information packet. We also summarizes the main link performance prediction techniques and in particular the κESM method, that is, how to predict the performance of the system when a certain setting of transmission parameters is employed for a given status of channel. Finally, the chapter introduce the *Goodput* (GP) as figure of merit, define as the number of information bit delivered in error free packets per unit of time.

2.1 Transmitter structure

This section describes the BIC-OFDM system based on the packet and frame processing and transmitting over a band B composed of N subcarriers belonging to the set of $D_s \triangleq \{1, \cdots, N\}$

2.2 SISO BIC-OFDM System Model

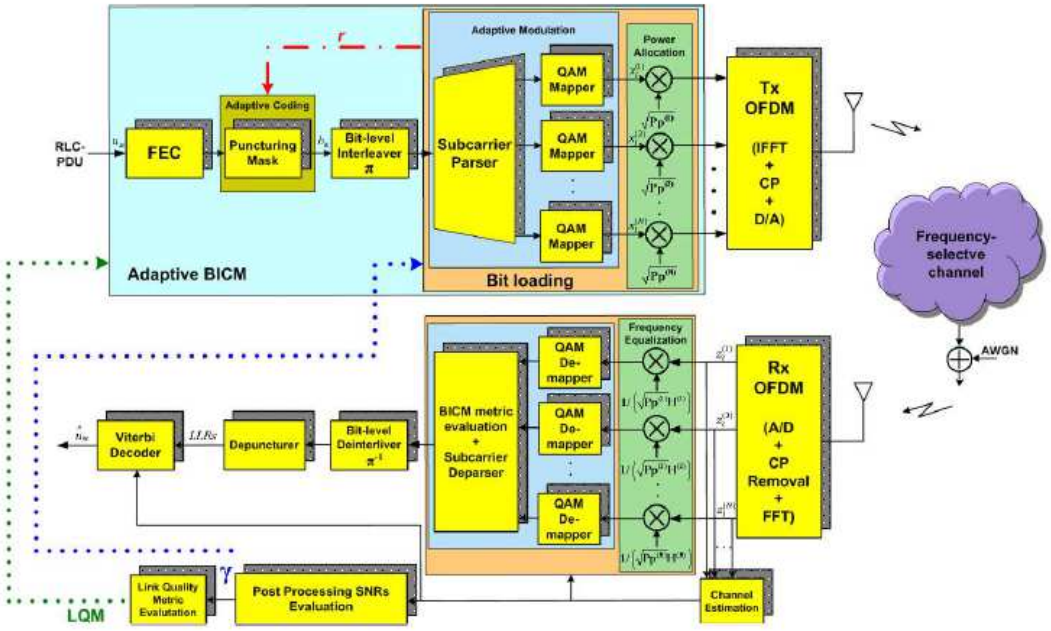

Figure 2.1: SISO-BIC-OFDM System Model.

Referring to the block diagram shown in Figure 2.1, each packet, identified by a RLC-PDU made of $N_u = N_h + N_p + N_{CRC}$ bits, i.e., including the header, the payload and the CRC section of size N_h, N_p, N_{CRC}, respectively, is transmitted through L consecutive OFDM symbols, which form an OFDM frame (or block). All the OFDM symbols, belonging to the same frame, experience the same fading realization. Each RLC-PDU is processed in two steps. In the first, called packet processing step, the RLC-PDU is input to the channel encoder. The N_u bits are encoded by a turbo coder, then punctured to obtain a certain code rate r. The code rate r is chosen in the set of punctured rates $D_r \triangleq \{r_0, \cdots, r_{max}\}$, where r_0 is the mother code rate and r_{max} the minimum code rate. The

resulting block consist of $N_c = N_u/r$ *coded binary simbols* (CBS) b_k, which are subsequently randomly interleaved. The bit-level interleaver randomly maps the generic CBS b_k, onto one of the label bits, carried by the symbols of the OFDM subcarriers, according to the follow notation:

$$b_k \rightarrow c_{\Pi(k)}, \tag{2.1}$$

$\Pi(k) \triangleq \{l_k, n_k, i_k\}$ is the interleaver law, which maps the index k of the CBS into a set of three coordinates:

1. l_k, the position of the OFDM symbol within the frame;
2. n_k, the OFDM subcarrier number;
3. i_k, the position of the cbs within the label of the QAM symbol on a certain subcarrier.

The interleaver is assumed to be fully random, so that the probability of mapping the generic CBS b_k into the i-th label bit of the QAM symbol transmitted on the n-th subcarrier into the l-th OFDM block denoted as $c_{l,n,i,}$ with $l = 1, \ldots, L$, $n = 1, \ldots, N$ and i = $1, \ldots, m_n$, is

$$\Pr\{b_k \rightarrow c_{l,n,i}\} \triangleq \frac{1}{Nc} \tag{2.2}$$

In the frame processing that follows, the coded information is mapped onto the physical resources available in the time-frequency grid. With m_n we denote the number of CBS, allocated on the n-th subcarrier. In detail, the interleaved sequence of CBS is broken into subsequences of m_n bits each, wich are Gray mapped onto the unit-energy symbols $x_n \in$ 2^{m_n}-QAM constellation, with $m_n \in D_m =\{2, 4, 6\}$. This means that the index k of CBS b_k is one-to-one mapped into a set of two coordinates (i_k, n_k), that is, b_k occupies the i_kth position within the label of the 2^{m_n}-QAM symbol sent on the n_k subcarrier. The modulation symbols are

re-arranged into the vector $\mathbf{x} \triangleq [x_1, \cdots, x_N]$ and allocated over the N available subcarriers along with a certain amount of power $\mathbf{p} = \triangleq [p_1, \cdots, p_N]$, where p_N denotes the power load over the nth subcarrier, and satysfing

$$\sum_{n=1}^{N} p_n \leq P \tag{2.3}$$

with P the available power in transmission. The process of power and bits distribution (among the subcarriers with a certain criterion) is called *Bit loading*. At this point, the data-bearing QAM symbols are transmitted, after having been subjected to the digital OFDM processing, including:

- IFFT;
- addiction of cyclic prefix (CP);
- Digital to Analog (D/A) conversion.

Then, the obtained signal is up-converted at carrier frequency f_c and transmitted over a frequency selected channel

2.3 Medium Structure

In a mobile-radio scenario, signals experience several degradation factors due to reflection, diffraction, scattering and, in general, to any obstacle that obstruct the line-of-sight (LOS) between transmitter and receiver. This phenomenon is called multipath fading. As a result, the receiver sees the superposition of multiple copies of the transmitted signal, each traversing a different path. Each signal copy will experience differences in attenuation, delay and phase shift while travelling from the source to the receiver. This can result in either constructive or destructive interference,

amplifying or attenuating the signal power seen at the receiver. Moreover, another significant effect is the time variation in the structure of the medium. As a results, the characteristics of the paths experienced by the transmitted signal can vary during time [2]. Statistical models for the channel impulse response of a fading multipath channel have been described in literature over the past years [3]. We define the coherence time T_C of the channel as the measure of the minimum time required for the magnitude change to become uncorrelated from its previous value. Since we suppose time T_C of the channel is much greater than the OFDM symbol duration T_S, the channel is affected by slowly-fading and the multipath parameters may be regarded as approximately invariant over many signaling intervals or for all the entire packet transmission. This model is called block-fading frequency selective channel and, accordingly, the channel impulse response can be expressed as

$$c(\tau) = \sum_{n=1}^{N_{pt}} c_n \delta(\tau - \tau_n), \tag{2.4}$$

where:

- N_{pt} is the channel length;
- c_n is the complex-valued channel;
- τ_n is the delay relevant on the nth path.

Even all these parameters are obviously random variables (RVs), the statistical models typical adopted for their characterization assume N_{pt} and τ_n fixed, whereas c_n are considered uncorrelated complex-valued Gaussian RVs. In particular, the variance of each coefficient c_n and the value of N_{pt} and τ_n are given by a power-delay profile of the model chosen. We will refer to ITU multipath fading models as specified in [4]

2.4 Reciever structure

At the receiver side, the signal will go through the whole inverse OFDM processing, in order to be coherently demodulated, subcarrier per subcarrier, exploiting the channel estimation, which will be assumed perfect. In particular, the signal passes trough:

- the analogic-to-digital converter;
- the CP removal;
- the serial-to-parallel (S/P) converter;

The resulting signal samples are input to the discrete Fourier Transformer (DFT) block. The model of the signal samples at the output of the DFT block results

$$z_n = \sqrt{p_n} x_n h_n + w_n, \quad \forall\ n \in D_s \tag{2.5}$$

where:

- h_n is the complex-valued channel coefficient on subcarrier n, that is obtained as the nth coefficient of the DFT of the channel response (2.4), encompassing also the transmitter and receiver filter;
- $w_n \in \mathcal{CN}(0, \sigma_n^{(w)^2})$ is the circular-symmetric complex-Gaussian random variable with standard deviation $\sigma_n^{(w)}$, denoting the thermal noise sample on subcarrier n.

The instantaneous post processing SNR values are then defined as

$$\gamma_n = p_n \frac{|h_n|^2}{\sigma_n^{(w)^2}}, \quad \forall\ n \in D_s \tag{2.6}$$

Finally, the receiver performs the soft metric evaluation, followed by de-interleaving and turbo decoding. In particular, the soft metric at the

input of the turbo decoder , identified by the log-likelihood ratio (LLR) of the kth coded binary symbol is expressed by

$$\Lambda_k = \log \frac{\sum_{\tilde{x} \in \chi_{b'_k}^{(i_k,n_k)}} p\left(z_{n_k} | x_{n_k} = \tilde{x}, \gamma_{1,\cdots,N}\right)}{\sum_{\tilde{x} \in \chi_{b_k}^{(i_k,n_k)}} p\left(z_{n_k} | x_{n_k} = \tilde{x}, \gamma_{1,\cdots,N}\right)} \tag{2.7}$$

where

$$p\left(z_{n_k} | x_{n_k} = \tilde{x}, \gamma_{1,\cdots,N}\right) \propto \exp\left(-\left|z_{n_k} - \sqrt{\gamma_{n_k}}\tilde{x}\right|^2\right) \tag{2.8}$$

is the Gaussian-shaped probability density function (p.d.f.) of the received sample value, conditioned on the transmitted symbol $\tilde{x}$ and on $\gamma_{1,\cdots,N}$, $\chi_a^{(i,n)}$ represents the subset of all symbols belonging to the modulation adopted on the nth subcarrier whose ith label bit is equal to a and b'_k denotes the complement of bit b_k.

2.5 Link Resource Adaptation

Adaptive Modulation and Coding (AMC) enables robust and spectrally-efficient transmission over time-frequency selective channels by making the best use of available resource. In fact, when a system does not adapt the transmission parameters to the actual channel conditions, the designer must consider a fixed link margin, to maintain an acceptable performance in the worst case channel conditions. The AMC design problem is essentially an optimization task with objective functions and constraints properly defined, so as to accommodate specific system scenarios. Each AMC strategy is characterized by an adaptation criterion (e.g. objective function), the target GP parameters (e.g. the constraints of the problem), the available information on the channel status, and the resulting output, which is represented by a set of optimized transmission parameters. The feasibility of this method, however, requires that the transmitter can perform precise and simple evaluation of the actual link

performance, in particular an accurate prediction of the *Packet Error Rate* (PER). It is well known that PER link performance, of a given coded digital communication over a stationary *Additive White Gaussian Noise* (AWGN) channel, can be expressed as a function of the *Signal To Noise Ratio* (SNR).

In multi-carrier systems such as *Orthogonal Frequency Division Multiplexing* (OFDM), however, the frequency selective fading over the transmission channel, introduces large SNR variations across the subcarriers, thus making link PER prediction a demanding task. The need of an accurate yet manageable link level performance figure has led to the *Effective SNR Mapping* (ESM) concept, where the vector of the received SNRs across the subcarriers is compressed into a single SNR value, which in turn can be mapped into a PER value.

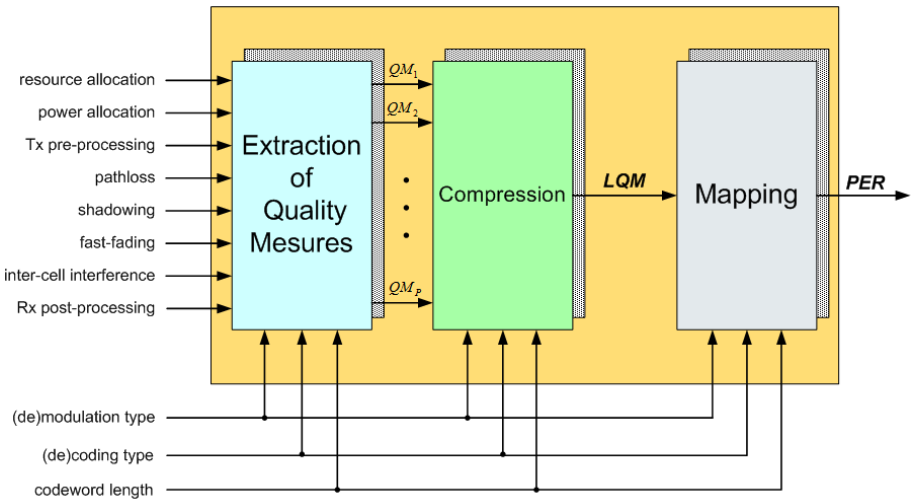

Figure 2.2: Structure of a generic link performance prediction model

We try to understand the general steps of the ESM by the Figure 2.2:

1. Extraction of a set of Quality Measures ($QM_p, p = 1, ..., P$), one for each resource element involved in the packet of interest;

2. The number of resource elements is generally very large (i.e. the number of subcarrier of an OFDM system), a compression over these amounts is required, massively reducing the number of quality measures to typically one: a scalar *Link Quality Metric* LQM;

3. This scalar is mapped to a PER value.

The objective of this method is to find a compression function, which maps a sequence of SNRs into a single value, that is strongly correlated with the actual PER. The basic principle of ESM is to be able to go from an instantaneous channel state (such as the instantaneous SNR for each subcarrier in the case of OFDM) to a corresponding PER, through a compressed value, called, as said, *effective* SNR and tagged in the sequel as $\hat{\gamma}_{eff}$. This is used to find an estimate of the PER from a basic AWGN link level performance.

For instance, given the set of the instantaneous post-processing SNRs experienced by the subcarriers of a OFDM system:

$$\gamma = \left[\gamma^{(1)}, \gamma^{(2)}, \ldots, \gamma^{(N)}\right] \tag{2.9}$$

with N the maximum number of subcarriers. From the knowledge of (2.9), we want to obtain the following result:

$$PER_{AWGN}(\hat{\gamma}_{eff}) = PER(\gamma) \tag{2.10}$$

where PER_{AWGN} and PER refer to the AWGN equivalent system and the one to be modelled, respectively. Depending on the way the compression function is derived, several ESM method technique have been proposed so far [5]

- The exponential ESM (EESM)[6] exploits an exponential function to obtain a rather simple but effective evaluation of link PER performance but only for the case of binary signalling. For high order

modulations it is necessary a fine tuning factor for adjusting the PER estimate and reaching good accuracy for each modulation and coding scheme.

- The capacity ESM [7], [8] yields an optimistic estimate of the real PER function of a link channel realization, since the actual information between transmitter and receiver on every subcarrier is upper bounded by the concerning capacity expression.

- The last solution makes up for this coarse approximation using a mutual information approach and so it is referred to as mutual information ESM (MIESM) [9], [10]. Differently from the other ones, it includes two separate models, one for the modulation and the other for the coding, thereby providing good prediction performance for the mixed-modulation as well. Therefore, such a separate modulation and coding model makes radio resources management like power allocation and rate adaptation very convenient, as done in [11]. Unfortunately, a closed expression for calculating the mutual information doe not exist, so a polynomial approximation is essential, as proposed in [10].

Finally, a novel ESM technique is represented by the model whose compression function is based on the cumulant moment generating function (CMGF) of the bit level log-likelihood metrics (2.7) at the input of soft decoder [12]. This method, called κESM for short, offers several significant features compared with existing ESM techniques, such as:

- improved accuracy performance compared with the conventional EESM method;

- separation of the modulation and coding models, thus making configurations using mixed modulation among subcarriers easy to man-

age;

- the use of a tuning factor (required for turbo codes) to offer even improved accuracy that is independent of the modulation format adopted on each subcarrier;

- similar accuracy (or even better for multi-level QAM modulations) as the MIESM method, while offering (unlike the MIESM) a modulation model with a convex and simple closed-form mapping function.

Thus, in the reminder of this thesis, wherever required, we will rely on the κESM model as link performance prediction method and, therefore, before proceeding further, its structure is briefly recalled in the following section.

2.5.1 The κESM model

This method relies on an accurate evaluation of the *Packet Error Probability* (PEP) through the statistical description of the BIC loglikelihood metrics, thus offering an efficient accuracy versus manageability trade-off. To identify the essentials of this ESM approach, let's first consider two distinct codewords $\mathbf{b} = [b_1, \cdots, b_d]^T$ and the competitor codeword $\mathbf{b}^{'} = [b'_1, \cdots, b'_d]^T$, both originated from the same state of the trellis code and merging after d steps. Denote with $\hat{\mathbf{b}}$ the corresponding decoder output, and then focus on the calculation of the PEP between $\mathbf{b}$ and $\mathbf{b}'$, namely $PEP(d) = \Pr\{\widehat{\mathbf{b}} = \mathbf{b}'|\mathbf{b}, \Upsilon\}$ with Υ is the diagonal matrix whose generic entry collects the square-roots of the post-procesing SNRs for the subcarriers. We review hereafter a basic approximation employed in the error probability analysis for BIC-modulation linear binary codes, and apply them to the case of interest: the so calles *Gaussian approximation*.

In fact, it is shown that: i) the tail of the distribution for the a-posteriori *LogLikelihood Ratio* (LLR) is well approximated by a Gaussian function, and ii) the decay of the *Bit Error Rate* (BER) for increasing SNR has an exponential nature. Starting from these results, let us now recall that in our LRA problem, we are focusing on the event of successfully receiving an entire packet without error and not a single bit. Hence, since we are interested in the delivery of error-free data packets, we aim at operating in a SNR region, in which the PER is lower than 1, which entails a low-to-medium BER value, namely just the region where the Gaussian approximation holds tight. Thus, with the assumptions of ideal random interleaving together with perfect CSI and assuming that the set of active subchannels can be schematized as a memoryless *Binary Input Output Symmetric* (BIOS) channel, the PEP can be computed as the tail probability.

$$PEP(d) \simeq Q(\sqrt{-2d\kappa_{\mathcal{L}}(\hat{s})}) \tag{2.11}$$

where $\kappa_{\mathcal{L}}(s) \triangleq \log \mathcal{M}_{\mathcal{L}}(s)$ is the Cumulant Generating Function (c.g.f.), $\mathcal{M}_{\mathcal{L}}(s) \triangleq E\{e^{s\mathcal{L}}\}$ is the *Moment Generating Function* (MGF) and $\hat{s}$ is the so-called "saddlepoint", which is definded as the value for wich κ'($\hat{s}$)=0. For more details see [13]. The c.g.f. can be evaluated as follow:

$$\kappa_{\mathcal{L}}(\tilde{s}) \simeq \log \left(\frac{1}{\sum_{n=1}^{N} m_n} \sum_{n=1}^{N} \sum_{\mu=1}^{\sqrt{2^{m_n}}/2} \frac{\psi_{m_n}(\mu)}{2^{m_n-1}} \cdot e^{-\frac{\gamma_n (\mu \cdot d_{m_n}^{(min)})^2}{4}} \right), \tag{2.12}$$

where $d_{m_n}^{(min)}$ is the minumum Euclidean distance between the symbols of the 2^{m_n}-QAM constellation adopted on the nth subcarrier and $\psi_{m_n}(\mu)$ defines the number of symbols at distance $\mu d_{m_n}^{(min)}$ from the nearest neighbor in the complementary subset of the constellation. It can be noted that equation (2.11) corresponds to the PEP of an equivalent system with binary modulation (BPSK) that experiences a simple AWGN chan-

nel with SNR

$$\hat{\gamma} \triangleq -\kappa_{\mathcal{L}}\left(\hat{s}\right), \tag{2.13}$$

Hence, considering that the PER depends on the PEP(d) function, the performance of the BIC-OFDM system characterized by the post-processing SNRs diagonal matrix Υ are estimated evaluating the performance of the equivalent binary system over AWGN channel characterized by the SNR $\hat{\gamma}_{kESM}$, i.e.,

$$PER\left(\Upsilon\right) = PER_{AWGN}\left(\hat{\gamma}_{kESM}\right), \tag{2.14}$$

where PER_{AWGN} is the PER of the equivalent system over AWGN channel. In conclusion, the κESM approach is described by the scheme in figure (2.3), where the division of modulation and coding models is well evident.

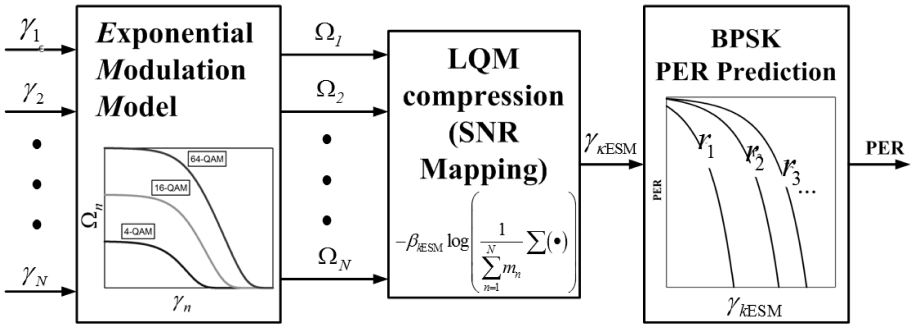

Figure 2.3: Structure of a generic link performance prediction model

In fact, is first evaluated the ESNR as

$$\hat{\gamma}_{kESM} \triangleq -\log\left(\frac{1}{\sum_{n=1}^{N} m_n}\sum_{n=1}^{N}\Omega_n\right), \tag{2.15}$$

where

$$\Omega_n \triangleq \sum_{\mu=1}^{\sqrt{2^{m_n}}/2} \frac{\psi_{m_n}\left(\mu\right)}{2^{m_n-1}} \cdot e^{-\frac{\gamma_n\left(\mu \cdot d_{m_n}^{(\min)}\right)^2}{4}}. \tag{2.16}$$

Defining

$$\alpha_{n,\mu} \triangleq \frac{\psi_{m_n}(\mu)}{2^{m_n-1}} \tag{2.17}$$

and

$$1/\rho_{n,\mu} = \frac{\gamma_n \cdot [d_{\min}^{(n,\mu)}]^2}{N_0} \tag{2.18}$$

we can finally write

$$\hat{\gamma}_{kESM} = -\log\left[\sum_{n=1}^{N}\sum_{\mu=1}^{\sqrt{2^m}/2}\frac{1}{m_n}\cdot\alpha_{n,\mu}\cdot e^{-(p_n/\rho_{n,\mu})}\right] \tag{2.19}$$

As apparent for (2.15)-(2.16), $\hat{\gamma}_{kESM}$, given the post-processing SNRs Υ, only depends on the modulation order adopted over each subcarrier and, besides, it is a convex function of the power allocation coefficients p_n, which are contained in γ_n via (2.6). Then $\hat{\gamma}_{kESM}$ is mapped into the PER value either entering into a LUT, where the values of the PER for all the considered coding rates are stored, or evaluating the PER via analytical models.

2.5.2 The Goodput Criteriation

Link resource adaptation strategies can be essentially described as constrained optimization problems. In fact, the optimization variables, i.e., the transmission parameters, must optimize a certain objective function, that describes the performance of the system, according to the available information and satisfy at the same time constraints on the required QoS. The output of this problem represents the setting of parameters to adopt during the transmission. A significative optimization criterion is represented by the GP, i.e., the number of data bits delivered in error-free packets per unit of time, or, offered layer 3 data rate. The GP approach allows to obtain a trade-off between data rate and link reliability. In

fact, in order to deliver a packet, the higher the data rate, the shorter the transmission time in one transmission attempt, but, more likely, the transmission will fail, thus engendering retransmissions. On the other hand, the more robust the transmission strategy, the more likely the packet will be delivered successfully within the retry limit, however, with less efficiency. Thus, a link adaptation strategy that maximizes the goodput optimally trades-off the probability that the packet will be delivered successfully and the shortest possible transmission time. Therefore, in the following, we will focus on the expected goodput (EGP) figure of merit, defined as the ratio of the expected delivered data payload and the expected transmission time.

Denoting ϕ_i the subspace containing all the allowed transmission mode ϕ_i at the i-th ARQ-PR, m_n, i and r_i the number of binary coded symbols transmitted on the subchannel n and the coding rate associated with the i-th protocol round, respectively, the number of RLC-PDU transmitted during an OFDM symbol period is given by:

$$\nu\left(\hat{\phi}_i\right) \triangleq r_i \sum_{n \in D_n} m_{m,i} \tag{2.20}$$

where $\hat{\phi}_i$ is the selected transmission mode. Since each RLC-PDU is composed by N_u bits and and the duration of its transmission is:

$$T_{PDU} = \frac{N_{PDU}}{\nu\left(\hat{\phi}_i\right)} T_{OFDM} \tag{2.21}$$

When the RLC-PDU is transmitted using the transmission mode $\hat{\phi}_i$ over the wireless channel condition summarized by the effective SNR value $\hat{\gamma}_{kESM}(\hat{\phi}_i)$ the probability of a successful frame transmission is:

$$P_{ACK}\left(\hat{\phi}_i\right) = 1 - PER\left(\hat{\gamma}_{\kappa ESM}\left(\hat{\phi}_i\right)\right) \tag{2.22}$$

where the ACK error probability has been neglected. Considering the entire RLC-PDU delivery process, with maximum number of transmission

attempts equal to p_{max} and denoting with $\hat{\phi} \in \Phi$ the vector representing the entire transmission strategy, where $\Phi = \Phi_0$ x Φ_1 x $\cdots$ x $\Phi_{p_{max}}$, the probability of a successful RLC-PDU delivery within the retry limit can be expressed as:

$$P_{succ}\left(\hat{\phi}\right) = 1 - \prod_{p=0}^{p_{\max}} \left[1 - P_{ACK}\left(\hat{\phi}_p\right)\right]. \tag{2.23}$$

Thus the average transmission duration for successful transmission is given by

$$D_{succ}\left(\hat{\phi}\right) = \sum_{p=0}^{p_{\max}} \frac{P_{ACK}\left(\hat{\phi}_p\right) \prod_{j=0}^{p-1}\left[1 - P_{ACK}\left(\hat{\phi}_j\right)\right]}{P_{succ}\left(\hat{\phi}\right)} \sum_{\mu=0}^{p} \left(T_{PDU}\left(\hat{\phi}_\mu\right) + T_{WAIT}\left(\hat{\phi}_\mu\right)\right), \tag{2.24}$$

where $\mathrm{T}_{WAIT}(\hat{\phi}_i)$ represents the waiting time before the pth transmission attempt. On the other hand, the time wasted for the transmission of unsuccessfully delivered packets is

$$D_{fail} = \sum_{\mu=0}^{p_{\max}} \left(T_{PDU}\left(\hat{\phi}_\mu\right) + T_{WAIT}\left(\hat{\phi}_\mu\right)\right). \tag{2.25}$$

Recalling that the average goodput is defined as ratio of the expected delivered data payload to the average transmission time, we have

$$GP\left(\hat{\phi}\right) = \frac{N_p}{\sum_{k=0}^{\infty}\left[\left(1 - P_{succ}\left(\hat{\phi}\right)\right)^k P_{succ}\left(\hat{\phi}\right)\left(kD_{fail}\left(\hat{\phi}\right) + D_{succ}\left(\hat{\phi}\right)\right)\right]}. \tag{2.26}$$

In order to simplify this expression, let us note that, when $p_{max} \to \infty$, then $P_{succ}(\hat{\phi}) \to 1$. As a consequence, assuming a number of maximum retransmission sufficiently large, using (2.22), we can approximate the goodput expression as

$$GP\left(\hat{\phi}\right) \simeq \frac{N_P}{\sum_{p=0}^{\infty} P_{ACK}\left(\hat{\phi}_p\right) \prod_{j=0}^{p-1}\left[1 - P_{ACK}\left(\hat{\phi}_j\right)\right] \sum_{\mu=0}^{p}\left(T_{PDU}\left(\hat{\phi}_\mu\right) + T_{WAIT}\left(\hat{\phi}_\mu\right)\right)} \tag{2.27}$$

The goodput expression in (2.27) needs to be further approximated in order to render it more manageable. We begin by making two simplifications:

- We assume to deal with continuous transmission (multiple SAW, SR), so that $\mathrm{T}_{WAIT}(\hat{\phi}_i)= 0$;
- At the generic ith protocol round, we know the current channel status only, while we assume not to be able to predict the future channel conditions.

So, we base the selection of the transmission mode under the assumption that the channel will remain the same along all the retransmission occurred on a certain packet, leading to:

$$\hat{\phi}_i = \phi \quad \forall i. \tag{2.28}$$

Thus, after some manipulations over the (2.27), reminding the (2.22) and also using the series:

$$\sum_{k=0,1}^{\infty} k\alpha^k = \frac{\alpha}{(1-\alpha)^2} \quad , |\alpha|<1 \tag{2.29}$$

we obtain the following goodput formula:

$$\begin{aligned} GP(\phi) &= \frac{N_p}{\frac{T_{PDU}(\phi)P_{ACK}(\phi)}{1-P_{ACK}(\phi)} \sum_{i=0}^{\infty} (i+1)[1-P_{ACK}(\phi)]^{i+1}} = \\ &= \frac{N_P}{T_{PDU}(\phi)\frac{1}{P_{ACK}(\phi)}} = \\ &= \frac{N_p}{N_{PDU}T_{OFDM}} \cdot \nu(\phi) \cdot [1 - PER(\hat{\gamma}_{kESM}(\phi))] \quad \left[\tfrac{bit}{s}\right] \end{aligned} \tag{2.30}$$

Within the expression above we can identify the two parameters for which the GP represents the *compromise*, in fact:

- $\frac{N_p}{N_{PDU}T_{OFDM}}$ $\nu(\phi)$ are the average number of information bits per OFDM period;

- 1-PER($\hat{\gamma}_{kESM}$) represents instead the reliability of a successful transmission of these bits.

It is clear that, the more one of these two amounts increases, the other one reduces. Let us notice, that the objective function just obtained is relevant to an OFDM symbol transmission period, and this result is a direct consequence of a Block fading assumption. This means, assuming that the channel and consequently the transmission mode remain stationary for all the OFDM symbols within a packet transmission time, so that we could concentrate only over the generic OFDM symbol transmission period.

In our analysis, we refer to GP x OFDM symbol, defined as the average number of information bits belonging to error free packet per OFDM symbol, that is

$$\zeta(\phi) = GP[\phi] \cdot T_{OFDM} = \frac{N_p}{N_u} \cdot \nu(\phi) \cdot [1 - PER(\hat{\gamma}_{kESM}(\phi))] \quad \text{bit/OFDM-Symbol} \tag{2.31}$$

Moreover, we can include N_p and N_u into a single factor

$$\zeta_0 = N_p / N_u \tag{2.32}$$

since it remains constant for all the packets and for all the possible transmission modes. Then, reminding (2.20) $\zeta(\phi)$ is valuable as follow:

$$\zeta(\phi) = \zeta_0 \cdot r \cdot \sum_{n=1}^{N} m_n \cdot [1 - PER(\hat{\gamma}_{kESM}(\phi))] \qquad \text{bit/OFDM-Symbol} \tag{2.33}$$

Chapter 3

Power Allocation in Point-to-Point BIC-OFDM System

3.1 Introduction

The problem to solve is a constrained optimization problem. The goal is minimize the total power allocated on each subcarrier subject to a constraint on GP x OFDM symbol. In particular, we define the sum of the allocated power (TAP) as the optimization function, and the GP/OFDM symbol as the constraint function. A mathematical formulation of this problem is:

$$\begin{aligned} \text{minimize} \quad & \sum_{n=1}^{N} p_n \\ \text{subject to} \quad & \zeta(\mathbf{p}) = \overline{\zeta} \qquad (3.1) \\ & \sum_{n=1}^{N} p_n \leq P \qquad (3.2) \end{aligned}$$

where P is the maximum available power in transmission. We suppose to not take into account the total power constraint (3.2) for the moment, since we assume that the optimal TAP vector satisfying constraint (3.1) is such that (3.2) is satisfied too and that can thus be omitted from (3.1).

3.2 Bit Loading

The aim is to satisfy over the link a given QoS, expressed in terms of a target GP value $\bar{\zeta}$ (bit/OFDM symbol), saving much power as possible. To this end, the transmission parameters to set are the modulation order over the active subcarriers, coding rate and power allocation vector. It is worth pointing out that, even if uniform bit loading is employed, the choice of the active subcarriers entails a bit loading procedure, in that the bit allocation vector $\mathbf{m}$ will be such that its nth component is $m_n = m$ if n is an active subcarrier, $m_n = 0$ otherwise. Moreover, the bit loading and power allocation problem cannot be jointly addressed, since this problem would be NP-hard. Thus, considering a given choice of modulation order, i.e., bit-per-subcarrier m, and coding rate r, a given QoS constraint $\bar{\zeta}$ and the SNR vector γ, this problem can be efficiently tackled in two steps as follows.

For the first step, the bit loading procedure, originally proposed in [35], is applied with the set of feasible bit per subcarrier being $\mathcal{D}_{\mathrm{m}} = \{0, m\}$. As result, we get N bit allocation vectors $\{\mathbf{m}^{(n)}\}_{n=1}^{N}$, where $\mathbf{m}^{(n)}$ is the best bit allocation vector with n active subcarriers when SNR vector γ is experienced. If $\bar{N} \leq N$ is the lowest integer such that $rm\bar{N} \geq \bar{\zeta}$, the bit allocation vector turns to be $\mathbf{m} = \mathbf{m}^{(\bar{N})}$.

3.3 Power Allocation Problem Formulation

In the second step, the optimization variable is the PA vector **p**. The aim now is to minimize the TAP guaranteeing at the same time the QoS constraint, i.e., a value of GP $\bar{\zeta}$, as shown in (3.1) As seen in (2.5.2), the GP is define as the number of information bit delivered in error free packets per unit of time. In particular, in equation (3.1) appears the GP/OFDM symbol, defined as the average number of information bits belonging to error free packet per OFDM symbol. In this analysis, it's supposed to adopt the same modulation on each subcarrier, i.e., m_n=m $\forall\ n \in N$:

$$\sum_{n=1}^{N} m_n = N \cdot m \qquad \text{with m= numer of bits per simbol} \tag{3.3}$$

The expression of GP/OFDM symbol and $\hat{\gamma}_{kESM}$ seen in (3.1) and (3.4) respectively, became:

$$\zeta = \zeta_0 \cdot r \cdot N \cdot m \cdot \sum_{n=1}^{N} [1 - PER(\hat{\gamma}_{kESM})] \quad \text{bit/OFDMsymbol} \tag{3.4}$$

$$\hat{\gamma}_{kESM} = -\log \left[\frac{1}{N \cdot m} \cdot \sum_{n=1}^{N} \sum_{\mu=1}^{\sqrt{2^m}/2} \alpha_{n,\mu} \cdot e^{-(p_n/\rho_{n,\mu})} \right] \tag{3.5}$$

The problem (3.1) can be rewritten in an equivalent manner as follow:

$$\begin{aligned} &\text{minimize} \quad \sum_{n=1}^{N} p_n \\ \text{s.t.} \quad &\sum_{n=1}^{N} \sum_{\mu=1}^{\sqrt{2^m}/2} \alpha_{n,\mu} \cdot e^{-(p_n/\rho_{n,\mu})} = \xi. \end{aligned} \tag{3.6}$$

Proof

Observing the constraint problem (3.1), and in particular the constraint function, the term ζ_0 as a constant. So the constraint on the GP

x OFDM symbol ζ turns into a constraint on the PER function. The problem (3.1) becomes:

$$\begin{aligned} \min \quad & \sum_{n=1}^{N} p_n \\ \text{s.t.} \quad & PER(\hat{\gamma}_{\kappa\text{ESM}}) = 1 - \frac{\bar{\zeta}}{\zeta_0 \cdot r \cdot N \cdot m} \end{aligned} \tag{3.7}$$

The PER is valuable in two different ways:

- via lookup table;
- like a negative exponential function $e^{(-\sigma_0(\gamma-\gamma_0))}$;

A typical trend of PER vs SNR is shown in Fig. 3.1:

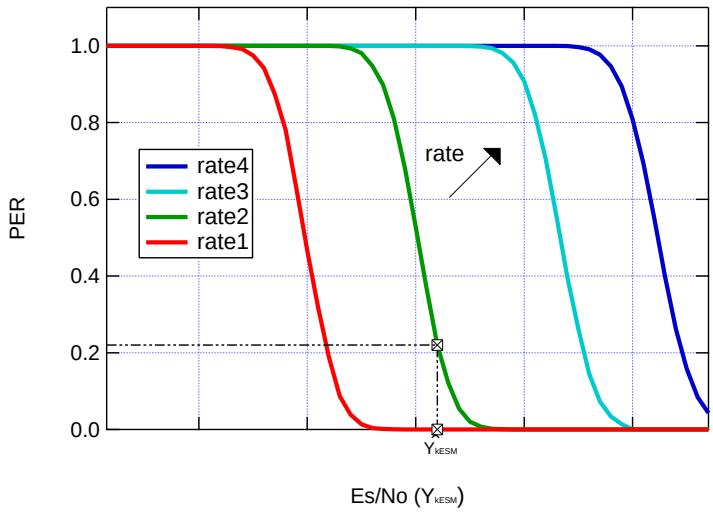

Figure 3.1: PER vs Es/No ($\hat{\gamma}_{kESM}$)

Because the exponential function is monotonically decreasing, as can be seen in Fig. 3.1, the constraint on PER function turns into a constraint on $\hat{\gamma}_{kESM}$. So (3.7) can be written as follow:

$$\hat{\gamma}_{kESM} = PER^{-1}\left(1 - \frac{\bar{\zeta}}{\zeta_0 \cdot r \cdot N \cdot m}\right) \tag{3.8}$$

We have to find $\hat{\gamma}_{kESM}$ such that:

$$\hat{\gamma}_{kESM}(\mathbf{p}) = \gamma_{opt} = PER^{-1}\left(1 - \frac{\bar{\zeta}}{\zeta_0 \cdot r \cdot N \cdot m}\right) \tag{3.9}$$

Replacing (3.4) in (3.9) yields:

$$-\log\left(\frac{1}{N} \cdot \sum_{n=1}^{N} \sum_{\mu=1}^{\sqrt{2^m}/2} \alpha_{n,\mu} \cdot e^{-(p_n/\rho_{n,\mu})}\right) = \gamma_{opt} \tag{3.10}$$

Finally, we can write the constrained problem as seen in (3.6):

$$\text{minimize} \quad \sum_{n=1}^{N} p_n$$

$$\text{s.t.} \quad \sum_{n=1}^{N} \sum_{\mu=1}^{\sqrt{2^m}/2} \alpha_{n,\mu} \cdot e^{-(p_n/\rho_{n,\mu})} = \xi \tag{3.11}$$

$$\text{with} \qquad \xi = e^{-\gamma^{opt}} \cdot N \cdot m \tag{3.12}$$

3.4 Solution analysis of the minimum power allocation's problem

Unfortunately, the solution of summation (3.6) is not calculable in a closed form because of the constraint (3.11). The only way to do that, is to put the term $\mu = 1$. As said before, this term depends on the modulation adopted on the transmission and on the distance between modulation's symbols. Choosing $\mu = 1$ is usually an approximation, except when the modulation is 4-QAM: in this case, the optimal solution of the constraint problem (3.6) is obtainable in a closed form. The problem is now to find a way to obtain the power allocated on each subcarrier p_n such that satisfies the constrain on GP using modulation like 16-QAM or 64-QAM. Solution is obtainable using the convex optimization theory,

and in particular the KKT conditions [16]. In fact, is demonstrable that the problem (3.6) is convex, independently of the value of μ. For this reason, we can certainly say that there is a solution, and this solution in unique.

3.4.1 First method: numerical

The first method to find a solution for (3.6) is to solve our problem numerically. This approach can be very heavy computationally and the results provided by that technique will be used as a benchmark for the alternative methods that we propose. The solution obtained by this method is optimal except by the intrinsic approximation introduced by the numerical method.

3.4.2 Second method

In this case, we stop the summation in (3.11) at μ= 1. Accordingly, the solution of (3.6) can be written as follows:

$$p_n^{mth2} = \rho_{n,1} \cdot \left[\log\left(\frac{1}{\lambda}\right) - \log\left(\frac{\rho_{n,1}}{\alpha_{n,1}}\right) \right]^+$$
$$\text{with} \quad \lambda \quad \text{such that} \quad \sum_{n=1}^{N} \alpha_{n,1} \cdot e^{-\left(p_n^{mth2}/\rho_{n,1}\right)} = \xi \tag{3.13}$$

We surely know that this solution is not optimal when 16-QAM or 64-QAM modulation are adopted. Solution is now achievable in a closed form and it will be a lower bound compared to the numerical optimal solution because of the approximation adopted:

$$\sum_{n=1}^{N} \alpha_{n,1} \cdot e^{-(p_n/\rho_{n,1})} \leq \sum_{n=1}^{N} \sum_{\mu=1}^{\sqrt{2^m}/2} \alpha_{n,\mu} \cdot e^{-(p_n/\rho_{n,\mu})} \tag{3.14}$$

3.4.3 Third method

Recalling (3.11), it can be demonstrated that:

$$\sum_{n=1}^{N}\sum_{\mu=1}^{\sqrt{2^m}/2}\alpha_{n,\mu}\cdot e^{-(p_n/\rho_{n,\mu})} \leq \sum_{n=1}^{N}(\alpha_{n,1}+\alpha_{n,2})\cdot e^{-(p_n/\rho_{n,1})} \tag{3.15}$$

Suppose then to solve problem (3.6) by using (3.15) as constraint function. Clearly, the solution is now achievable in a closed form and it will be an upper bound compared to the numerical optimal solution previously proposed.

$$p_n^{mth3} = \rho_{n,1}\cdot\left[\log\left(\frac{1}{\lambda}\right) - \log\left(\frac{\rho_{n,1}}{\alpha_{n,1}+\alpha_{n,2}}\right)\right]^+$$

$$\text{with} \quad \lambda \quad \text{such that} \sum_{n=1}^{N}(\alpha_{n,1}+\alpha_{n,2})\cdot e^{-\left(p_n^{mth3}/\rho_{n,1}\right)} = \xi \tag{3.16}$$

3.4.4 Fourth method

The idea is to modify (3.15) as follow:

$$\sum_{n=1}^{N}\sum_{\mu=1}^{\sqrt{2^m}/2}\alpha_{n,\mu}\cdot e^{-(p_n/\rho_{n,\mu})} \leq \sum_{n=1}^{N}(\alpha_{n,1}+\delta\cdot\alpha_{n,2})\cdot e^{-(p_n/\rho_{n,1})} \leq \sum_{n=1}^{N}(\alpha_{n,1}+\alpha_{n,2})\cdot e^{-(p_n/\rho_{n,1})} \tag{3.17}$$

where $0 \leq \delta \leq 1$

Solution now became:

$$p_n^{mth4} = \rho_{n,1}\cdot\left[\log\left(\frac{1}{\lambda}\right) - \log\left(\frac{\rho_{n,1}}{\alpha_{n,1}+\delta\cdot\alpha_{n,2}}\right)\right]^+ \tag{3.18}$$

The problem to find the δ_{opt} (optimum in the sense of minimizing the TPA) is solved referring to the optimal solution evaluated with the numerical method like follow:

$$\delta \quad \text{such that} \quad \sum_{n=1}^{N}(\alpha_{n,1}+\delta\cdot\alpha_{n,2})\cdot e^{-(p_n^{opt}/\rho_{n,1})} = \xi \tag{3.19}$$

where p_n^{opt} is the optimal PA evaluated with numerical method

Solving equation (3.19) with respect to δ (that is the only unknown parameter) give us δ_{opt}. Finally, we substitute this value in eq. (3.18) and get the PA in closed form solution of method 4.

3.5 Simulation Results

We now show some simulation results. This simulations are useful to assess the best method to solve problem (3.6) in closed form.

3.5.1 System Setup

The system used is a SISO BIC-OFDM, which has:

1. $N = 1320$ subcarriers;
2. 4-, 16- and 64-QAM as modulation format;
3. Cyclic prefix of length $N_{CP} = 160$ for the Pedestrian-B channel (see Tab. 3.2);
4. Signalling interval equal to $T = 50$ ns, corresponding to a bandwidth of $B = 20$MHz;
5. Channel encoding is based on a Turbo Encoder (TC) composed by two parallel convolutional encoder, with mother code rate r = 1/3 properly punctured to allow the eight rates 1/3, 2/5, 1/2, 4/7, 2/3, 3/4, 4/5 and 6/7;
6. Each RLC-PDU consists of $N_p = 1024$ payload binary information symbols, preceded by the CRC section of length $N_{CRC} = 32$;
7. The bitloading is uniform for every subcarrier.

The features of the simulator are:

- 10000 transmitted packets;
- Active Subcarriers = 64;
- min GP = 10, 20, 30 (for equivalent system with 64 Active Subcarriers) .

3.5.2 Evaluation of the δ factor

The objective is to find the optimal TAP with Numerical Method and use it to find the value of δ_{opt} for each possible modulation and coding adopted, as described in sec. (3.4.4). Showing the dependance of δ_{opt} from modulation and coding, we will write from now $\delta_{opt}^{m,r}$. The algorithm performs several steps to reach this purpose:

- as said in (3.7), a constraint on GP turns into a constraint on PER($\hat{\gamma}_{kESM}$). So, fixed the GP and the *number of active subcarriers* (NOAS) $N \in D_n$ with the *bitload algorithm*, we can find a value of $\hat{\gamma}_{kESM}$;
- with the knowledge of $\hat{\gamma}_{kESM}$, CSI and NOAS we can perform the PA with Numerical Method;
- fixed modulation and coding, the program exhaustively calculates all the PAs for all the possible configuration of active subcarriers (that satisfy the constraint on GP). From all of these configurations, we'll chose the one that minimize the TAP as seen in (3.1);
- from the knowledge of the power allocated on each subcarriers with Numerical Method p_n^{opt} we can solve (3.19) to find $\delta_{opt}^{m,r}$.

The values of $\delta_{opt}^{m,r}$ are shown in table (3.1):

Code Rate	4-**QAM**	16-**QAM**	64-**QAM**
1/3	0	0.3875	0.6744
2/5	0	0.2982	0.5198
1/2	0	0.1770	0.3125
4/7	0	0.1074	0.2500
2/3	0	0.0363	0.0856
3/4	0	0.0160	0.0364
4/5	0	0.0077	0.0180
6/7	0	0.0021	0.0050

Table 3.1: LUT for $\delta_{opt}^{m,r}$

Once we collects all the values of $\delta_{opt}^{m,r}$, we proceeded with the next clusters of simulation. Comparison between methods are proposed.

3.5.3 Numerical method vs second method

Simulation using matlab are then proposed. We compare the total allocated power (TAP) by method described in sec. (3.4.1) and sec. (3.4.2) on a BIC-OFDM transmission. Results is calculated fixing the performance (GP), code rate (r) and modulation (m) of the link and varying the distance between transmitter and receiver antenna.

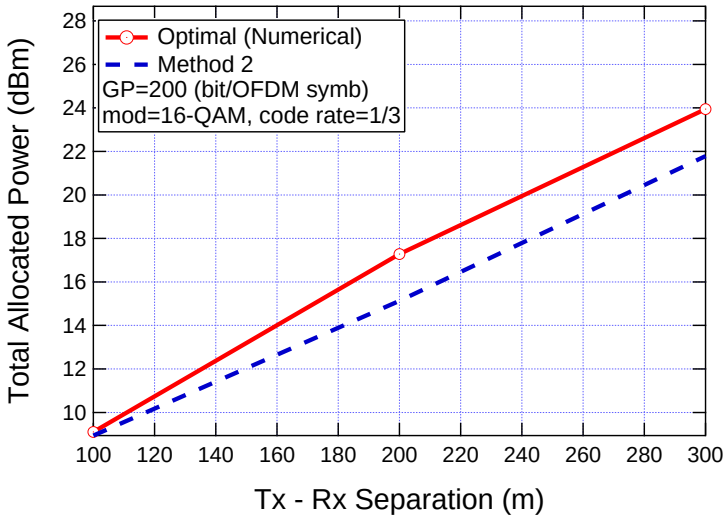

Figure 3.2: Total allocated power by numeric and second methods varying the distance: GP=200 bit/OFDM-Symbol, r= 1/3, mod= 16-QAM

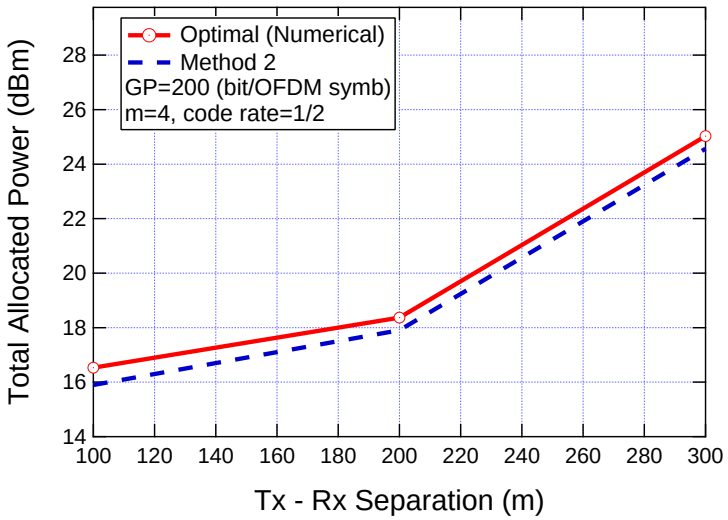

Figure 3.3: Total allocated power by numeric and second methods varying the distance: GP=200 bit/OFDM-Symbol, r= 1/2, mod= 16-QAM

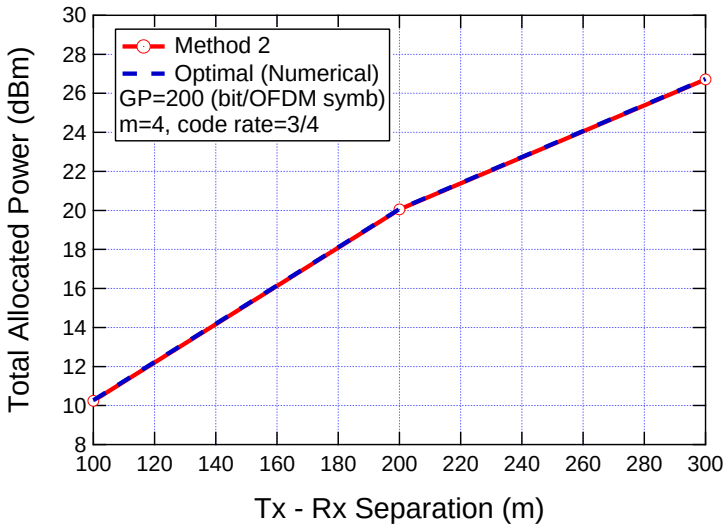

Figure 3.4: Total allocated power by numeric and second methods varying the distance: GP=200 bit/OFDM-Symbol, r= 3/4, mod= 16-QAM

As Fig. 3.2, 3.3 and 3.4 show, this second method tends to underrate the total power allocated respect the optimal numeric method, especially for low code rates (high redundance). This translates into the fact that the constraint on the GP will not be respected and the transmission doesn't reach the desired performance. This problem seems to disappear increasing the code rate (low redundance). As shown in (3.4), the two methods proposed are practically superimposed. This behavior doesn't change if we modify the modulation adopted as shown in Fig. 3.5, 3.6, 3.7.

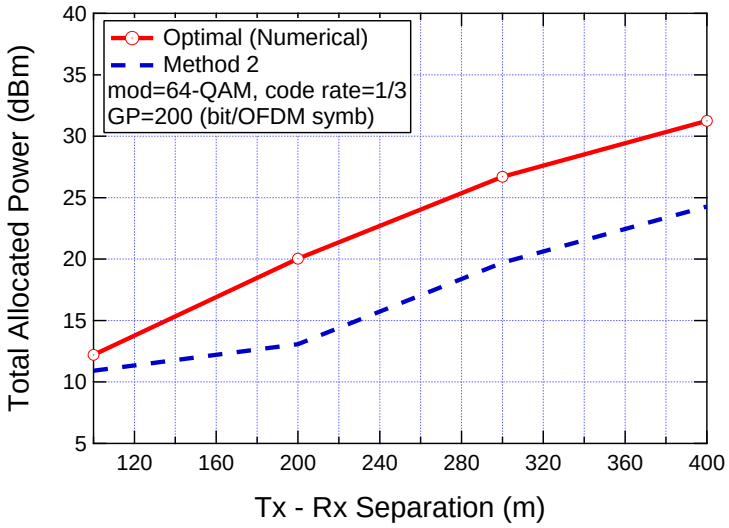

Figure 3.5: Total allocated power by numeric and second methods varying the distance: GP=200 bit/OFDM-Symbol, r= 1/3, mod= 64-QAM

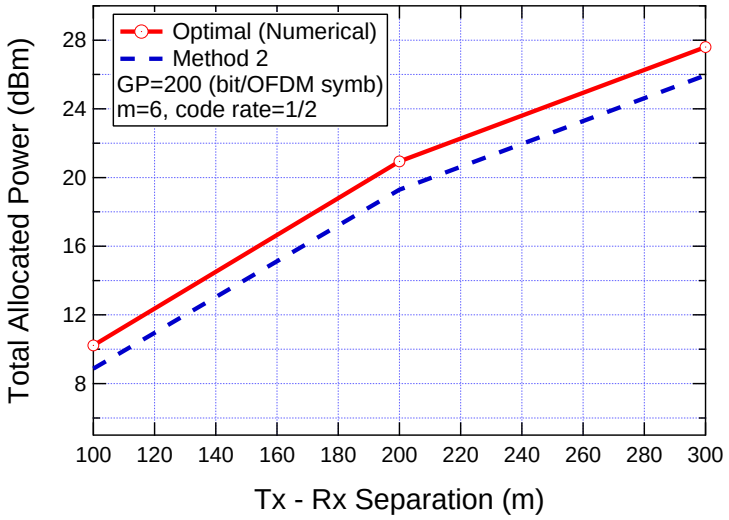

Figure 3.6: Total allocated power by numeric and second methods varying the distance: GP=200 bit/OFDM-Symbol, r= 1/2, mod= 64-QAM

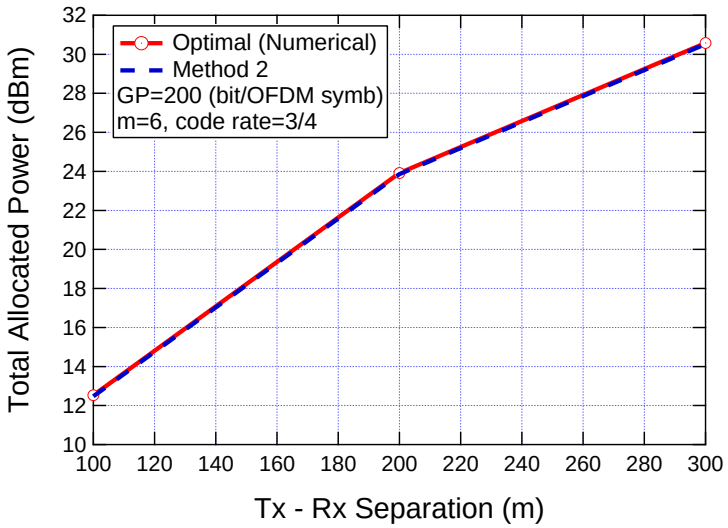

Figure 3.7: Total allocated power by numeric and second methods varying the distance: GP=200 bit/OFDM-Symbol, r= 3/4, mod= 64-QAM

or the constraint on GP (Fig. 3.8, 3.9, 3.10).

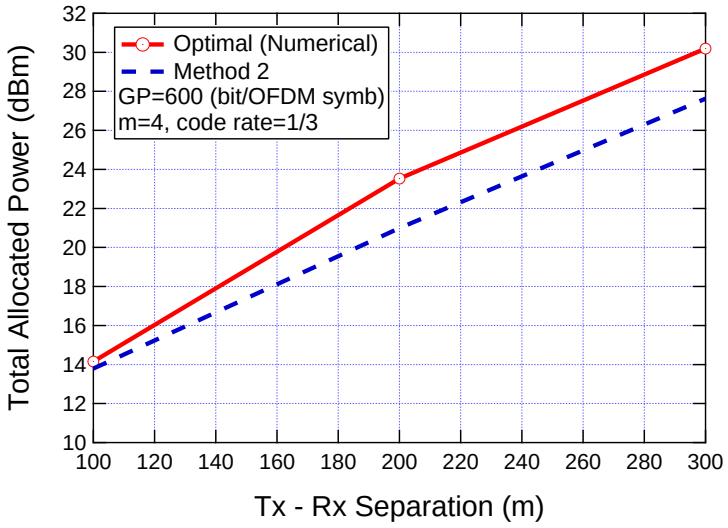

Figure 3.8: Total allocated power by numeric and second methods varying the distance: GP=600 bit/OFDM-Symbol, r= 1/3, mod= 16-QAM

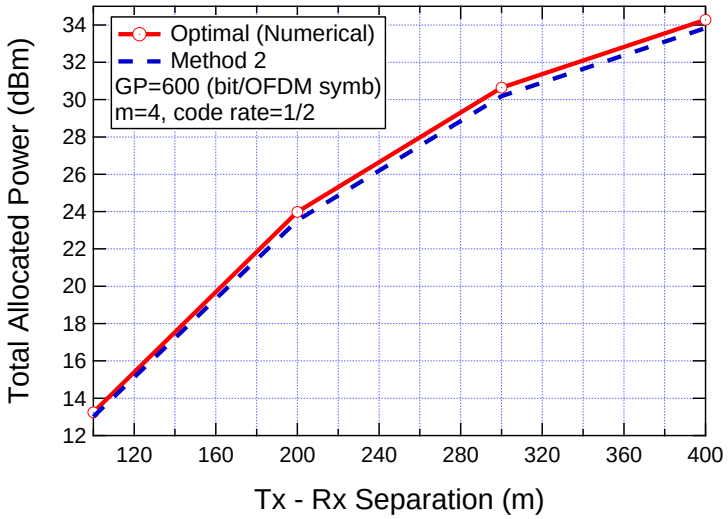

Figure 3.9: Total allocated power by numeric and second methods varying the distance: GP=600 bit/OFDM-Symbol, r= 1/2, mod= 16-QAM

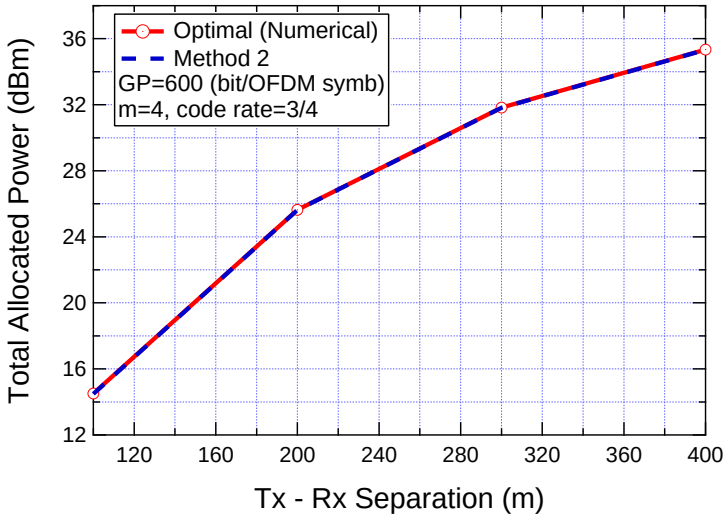

Figure 3.10: Total allocated power by numeric and second methods varying the distance: GP=600 bit/OFDM-Symbol, r= 3/4, mod= 16-QAM

Results show how the second method does not work properly for low

code rate. In fact, the power allocated in these cases is less than the necessary one and the performance fixed by the constraint on the GP are not satisfied. The situation gets better increasing the code rate, where the method closely follow the numerical optimal method. Second method's efficiency is independent from the constraint on GP selected.

3.5.4 Numerical method vs third method

Simulation using matlab and graphs are proposed comparing the TAP by method shown in Sec. 3.4.3 and Sec. 3.4.1 on a BIC-OFDM transmission. Results are calculated fixing the performance (GP), code rate (r) and modulation (m) of the link and varying the distance between transmitter and receiver antenna.

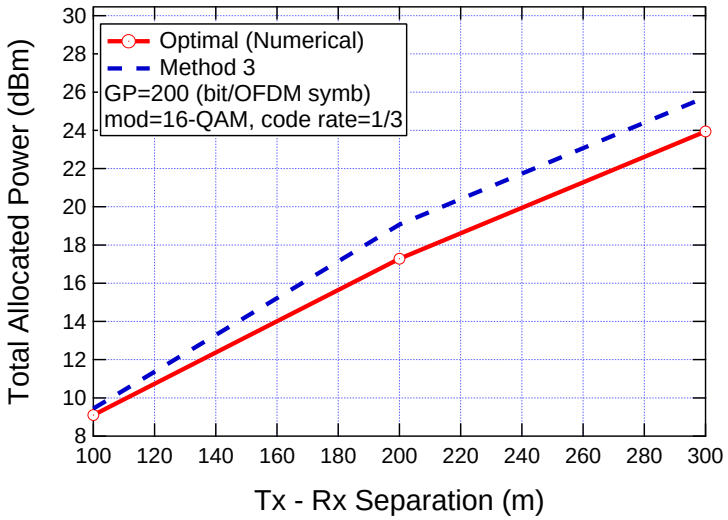

Figure 3.11: Total allocated power by numeric and third methods varying the distance: GP=200 bit/OFDM-Symbol, r= 1/3, mod= 16-QAM

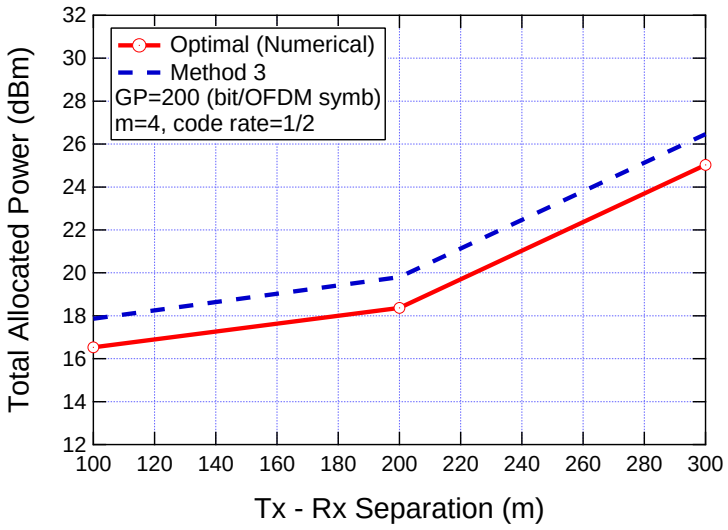

Figure 3.12: Total allocated power by numeric and third methods varying the distance: GP=200 bit/OFDM-Symbol, r= 1/2, mod= 16-QAM

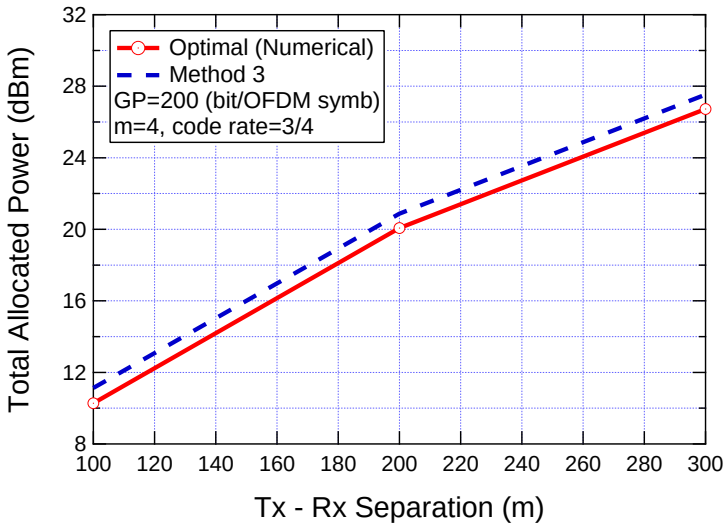

Figure 3.13: Total allocated power by numeric and third methods varying the distance: GP=200 bit/OFDM-Symbol, r= 3/4, mod= 16-QAM

Results for a 16-QAM modulation show what anticipated before:

third method tends to overestimate the TAP respect to the optimal value of the numeric method. This is the opposite behaviour respect the second method. In fact, if the TAP is overestimate, we surely reach the performance in term of GP, but we use more power than necessary. The situation remains the same chancing the code rate as shown in Fig. 3.11, Fig. 3.12 and Fig. 3.13. Changing the modulation, there are no improvements (Fig. 3.14, 3.15, 3.16):

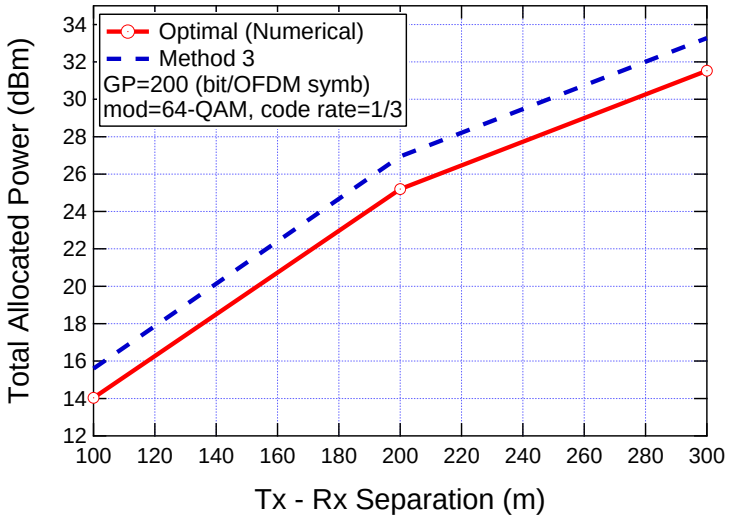

Figure 3.14: Total allocated power by numeric and third methods varying the distance: GP=200 bit/OFDM-Symbol, r= 1/3, mod= 64-QAM

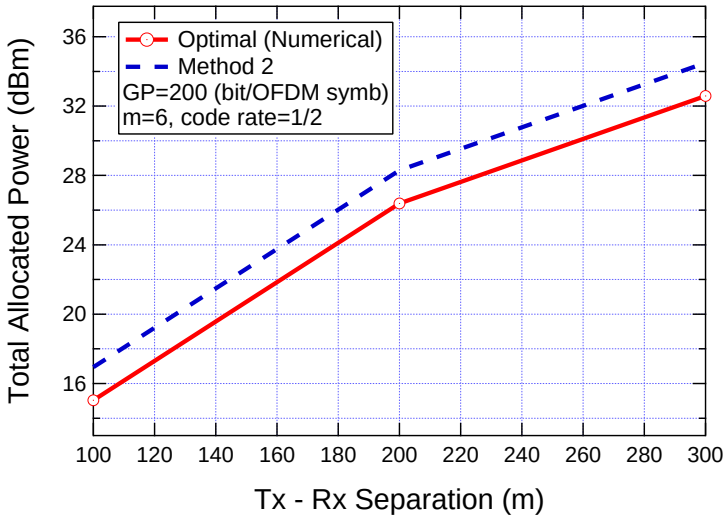

Figure 3.15: Total allocated power by methods varying the distance: GP=200 bit/OFDM-Symbol, r= 1/2, mod= 64-QAM

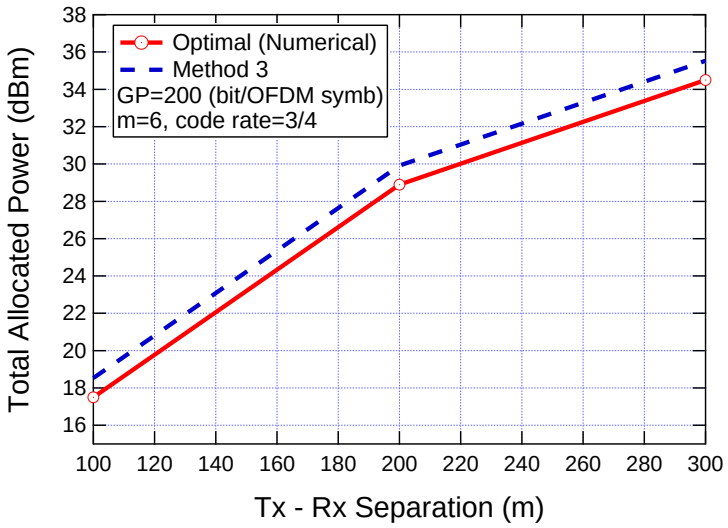

Figure 3.16: Total allocated power by methods varying the distance: GP=200 bit/OFDM-Symbol, r= 3/4, mod= 64-QAM

Results are conceptually the same as the 16-QAM. In conclusion,

third method overestimate the TAP. So, the performance are reached, but the power is not well-allocated. This tradeoff in independent of the GP selected as shown in Fig. 3.17:

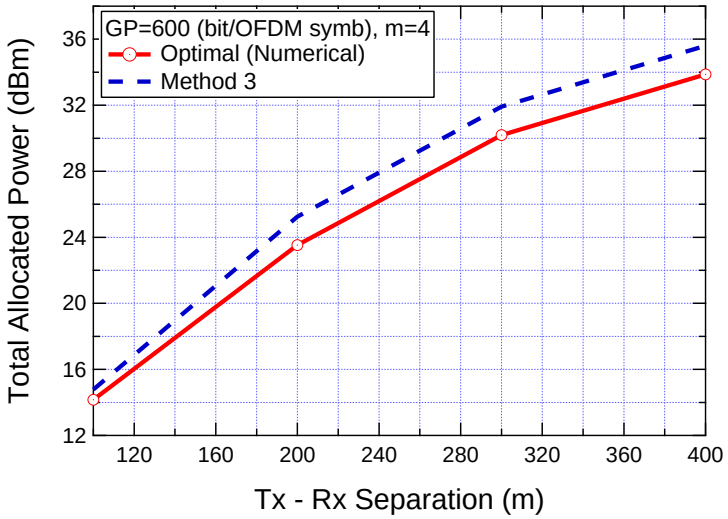

Figure 3.17: Total allocated power by numeric adn third methods varying the distance: GP=600 bit/OFDM-Symbol, r= 1/3, mod= 16-QAM

3.5.5 Numerical method vs fourth method

Simulation using matlab and graphs are proposed comparing the TAP by method (3.4.4) and (3.4.1) on a BIC-OFDM transmission. Results are calculated fixing the performance (GP), code rate (r) and modulation (m) of the link and varying the distance (so the SNRs) between transmitter and receiver antenna.

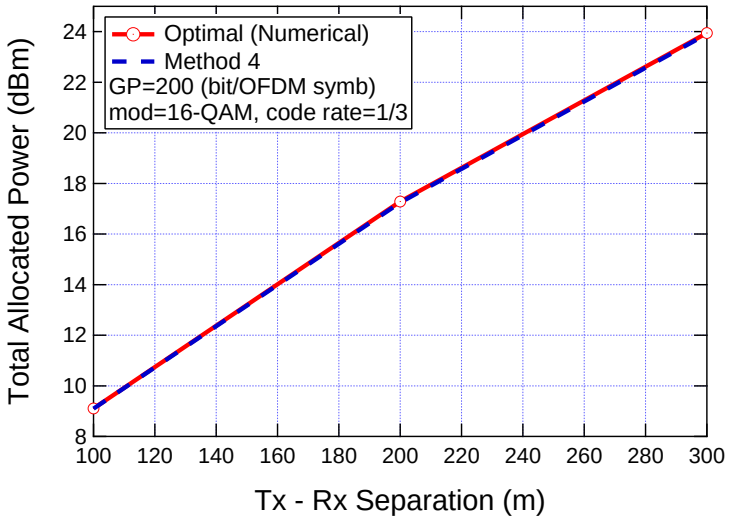

Figure 3.18: Total allocated power by Numerical and fourth methods varying the distance: GP=200, r= 1/3, mod= 16-QAM

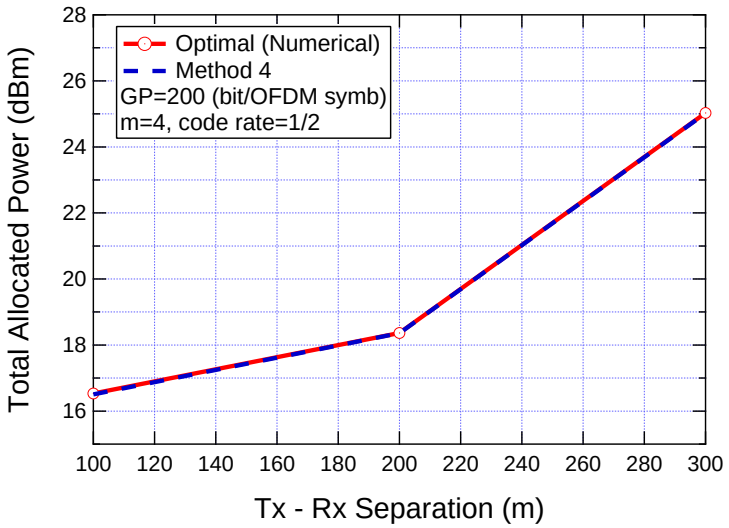

Figure 3.19: Total allocated power by Numerical and fourth methods varying the distance: GP=200, r= 1/2, mod= 16-QAM

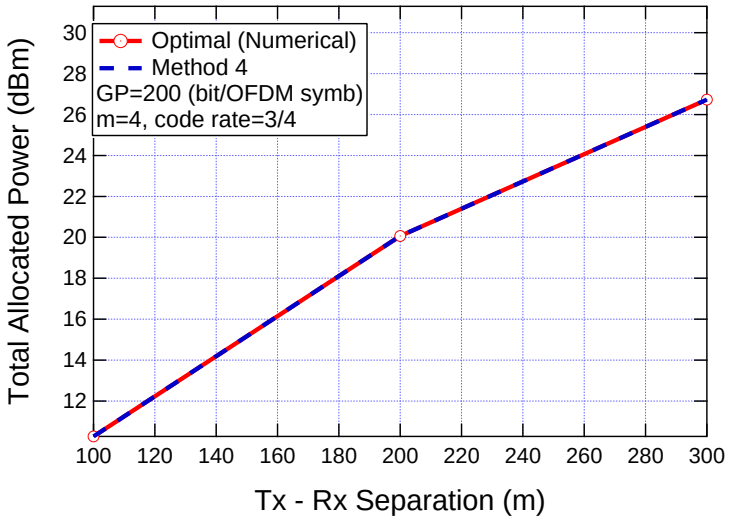

Figure 3.20: Total allocated power by Numerical and fourth methods varying the distance: GP=200, r= 3/4, mod= 16-QAM

As seen in Fig. 3.18, 3.19 and 3.20 , fourth method always follows the Numerical one for high and low redundancy code rate. Results do not change if we change the modulation adopted as shown in Fig. 3.21

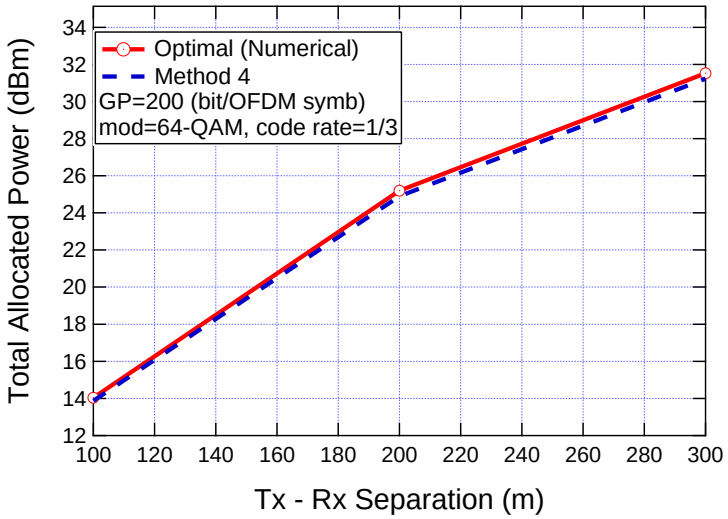

Figure 3.21: Total allocated power by Numerical and fourth methods varying the distance: GP=200, r= 1/3, mod= 64-QAM

or the constraint on GP as shown in Fig. 3.22

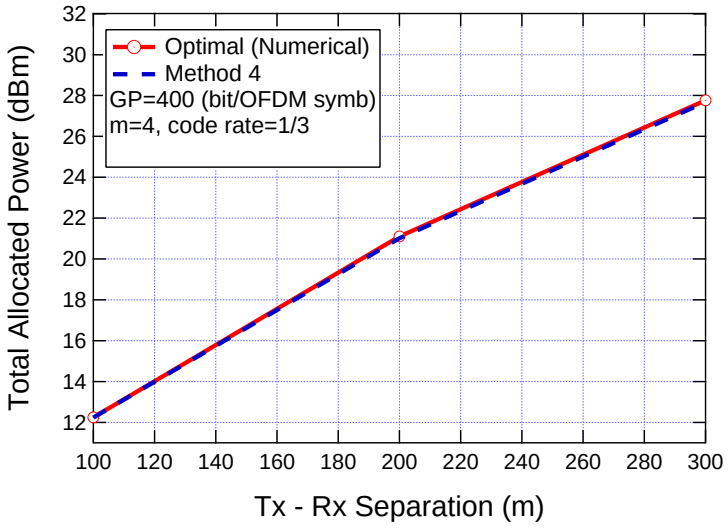

Figure 3.22: Total allocated power by Numerical and fourth methods varying the distance: GP=400, r= 1/3, mod= 16-QAM

3.5.6 Best method evaluation

A final comparison between the three methods proposed follows.

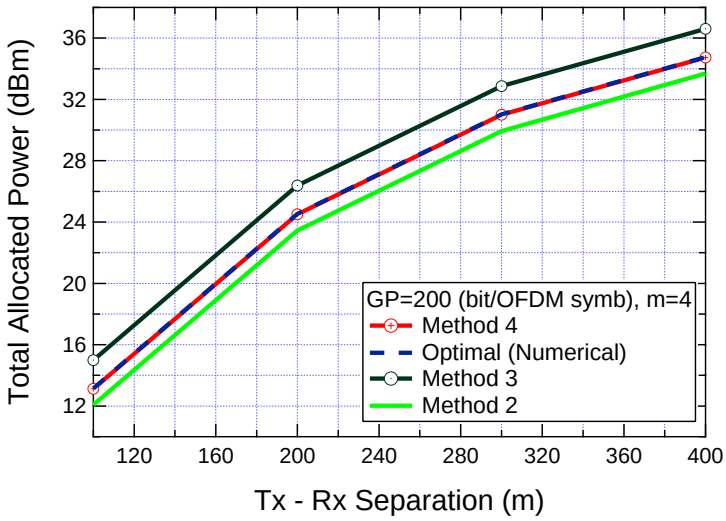

Figure 3.23: Confrontation between Numeric, second, third and fourth methods

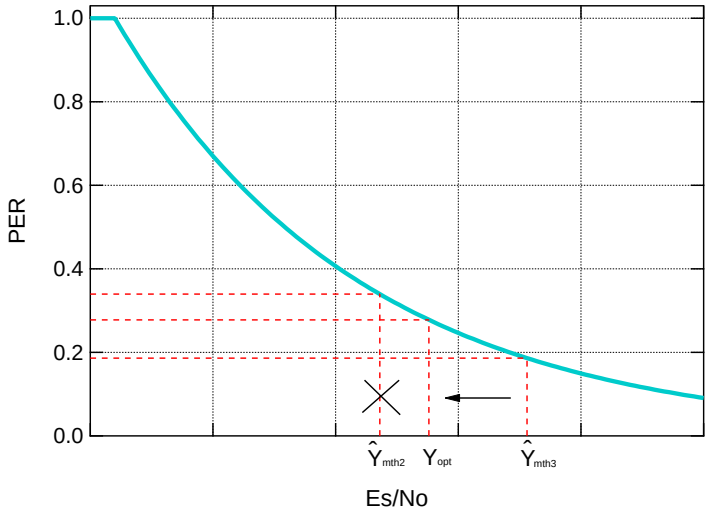

Figure 3.24: Dependence between PER and the $\hat{\gamma}_{kESM}$ estimation

As shown in figure (3.24) γ_{mth2} is a $kESM$ factor that not satisfied the constraint on the PER (and then on the GP). This means that the power allocated is not sufficient to reach the performance. Such $kESM$ factor is provided by the second method for low code rate as seen in (3.4.2). Conversely, $\hat{\gamma}_{mth3}$ is a $kESM$ factor that overestimate the PER. Such $kESM$ is provided by the third method as shown in (3.4.2). We want to start from such kESM ($\hat{\gamma}_{mth3}$) and move left on the x-asis of figure (3.24) trying to reach γ_{opt}. That's the description of the fourth method.

Observing the results, we can certainly say that:

- second method tends to underestimate the total power allocated for low code rate. For this reason, the constraint on the GP are not satisfied. The situation tends to get better increasing the code rate;
- third method always overestimate the power allocation. This method satisfy the constraint on the GP, but use more power than necessary and, because of this, does not suit our need to minimize the total power allocated
- fourth method always follow the numeric method, for any code rate, modulation and min GP selected. It's definitely the best of the three method to minimize the power allocated. The only disadvantage of such approach is that need to know p_n^{opt} for each subcarries. This value, as said, are necessary to estimate the δ_{opt} and are provided by the Numerical Method.

As shown in Fig. 3.18, 3.19 and 3.20, the fourth method works well for low and high code rate. This method works properly for any modulation adopted (16-QAM, 64-QAM), any code rate and any value of GP selected. From now we suppose to use this second method for our power analysis

and tag it as *Delta method* (DM). The advantage to know the value of δ_{opt} allow us to not evaluate the PA also with numerical method. It's important to know that δ_{opt} value is dependent on the modulation and coding selected for the transmission but is independent from the value of GP we want to reach. The next clusters of simulation we improved want to collect all the possible value of δ_{opt} and store it into a LUT.

3.5.7 Final simulation results

This time, the program implement a point-to-point SISO BIC-OFDM transmission using turbo code described in (2.1). The TAP algorithm exhaustively scans all the possible combination of modulation (selecting between 4-QAM, 16-QAM, 64-QAM) and turbo code rate and selects the combination mod/cod that satisfied the constraint on GP and at the same time allocates the minimum TAP. Obviously, we use DM as power allocation algorithm with the value of $\delta_{opt}^{m,r}$ previously calculated and stored in Tab. 3.1.

We then use this power allocation vector to the OFDM transmission. The simulation shows the behavior TAP varying the SNRs at the RX.

System Setup The system used is a SISO BIC-OFDM, which has:

1. $N = 1320$ subcarriers;
2. 4-, 16- and 64-QAM as modulation format;
3. Cyclic prefix of length $N_{CP} = 160$ for the Pedestrian-B channel (see table 3.2);
4. Signalling interval equal to $T = 50$ ns, corresponding to a bandwidth of $B = 20$MHz;
5. Channel encoding is based on a Turbo Encoder (TC) composed by two parallel convolutional encoder, with mother code rate r = 1/3

properly punctured to allow the eight rates 1/3, 2/5, 1/2, 4/7, 2/3, 3/4, 4/5 and 6/7;

6. Each RLC-PDU consists of $N_p = 1024$ payload binary information symbols, preceded by the CRC section of length $N_{CRC} = 32$;

7. The bitloading is uniform for every subcarrier.

Taps	**Relative Delay (ns)**	**Relative Power (dB)**
1	0	0.0
2	200	−0.9
3	800	−4.9
4	1200	−8.0
5	2300	−7.8
6	3700	−23.9

Table 3.2: ITU Pedestrian-B channel model

The features of the simulator are:

- Adaptive Modulation and Code (AMC) ;
- 10000 transmitted packets;
- Number of Subcarriers = 192;
- min GP = 10 (for equivalent system with 192 Subcarriers).

Results of simulation are shown in figure (3.25):

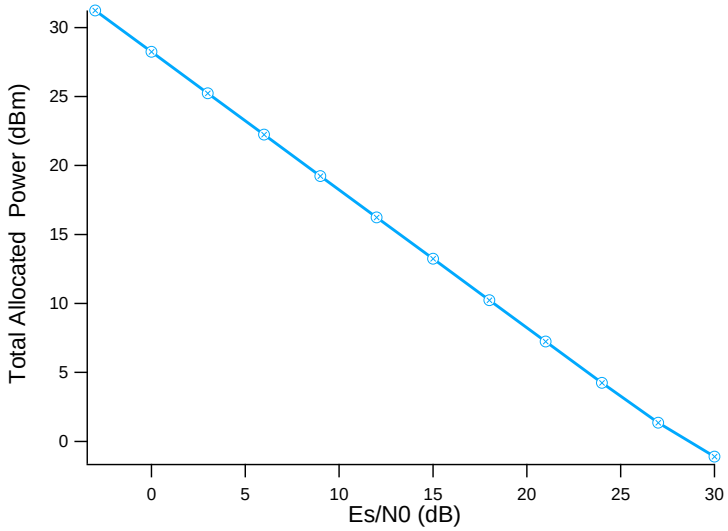

Figure 3.25: Total allocated power vs Es/N0 in a SISO BIC-OFDM transmission model

As we can see from figure (3.25), the algorithm is consistent. In fact, the more the Es/N_0 at receiver antenna is high, the less is the TAP necessary to satisfied the constraint on GP. It's important to note that, in a point-to-point communication as the one we have implemented, the AMC algorithm always chooses a 4-QAM modulation and a high redundance code rate (1/3) to minimize the TAP. The hypothesis of only one transmitter is obviously an ideal case. In all the radio communications there always more than one users that want to transmit over the same bandwidth. So, a few transmitter users can cause interference to each others. This kind of interference is called *Multiple User Interference* (MUI). Also, using a bigger modulation than the 4-QAM allows us to use a less NOAS. So, we can speculate that in certain particular situations it could be worth to use a bigger modulation, for example to reduce the MUI or for using a less amount of bandwidth for user. For this reasons, in Chapter 5 we tackle the problem seen in (3.1) in a multiuser small

cells scenario to analyze what kind of modulation is worth to adopt to minimize the TAP for each user. In the next chapter, instead, we will introduce a brief discussion about Game theory and Nash equilibrium to better understand such kind of transmission scenario.

Chapter 4

Game Theory

In this chapter it is provided a brief introduction to game theory that will form the basis of the next chapter.

4.1 Introduction

A game can be cooperative or noncooperative [21]. *Noncooperative game theory* refers to models in which each players are assumed to behave selfishly and their behaviors are directly modeled. *Cooperative game theory* which it is not cover here, generally refers to more abstract and axiomatic analyses of bargains or behaviors that players might reach, without explicitly modeling the processes [22].

The basic elements of performing a noncooperative game-theoretic analysis are framing the situation in terms of the actions available to players and their payoffs as a function of actions, and using various equilibrium notions to make either descriptive or prescriptive predictions. In framing the analysis, a number of questions become important. First, who are the players? They may be people, firms, organizations, governments, ethnic groups, and so on. Second, what actions are available to them? All actions that the players might take that could affect any

players payoffs should be listed. Third, what is the timing of the interactions? Are actions taken simultaneously or sequentially? Are interactions repeated? The order of play is also important. Moving after another player may give player i an advantage of knowing what the other player has done; it may also put player i at a disadvantage in terms of lost time or the ability to take some action. What information do different players have when they take actions? Fourth, what are the payoffs to the various players as a result of the interaction? Ascertaining payoffs involves estimating the costs and benefits of each potential set of choices by all players. In many situations it may be easier to estimate payoffs for some players (such as yourself) than others, and it may be unclear whether other players are also thinking strategically. This consideration suggests that careful attention be paid to a sensitivity analysis.

Once we have framed the situation, we can look from different players perspectives to analyze which actions are optimal for them. There are various criteria we can use.

4.2 Games in Normal Form

Let us begin with a standard representation of a game, which is known as a *normal form game*, or a game in *strategic form*:

- The set of players is $N = \{1, \ldots, n\}$.
- Player i has a set of actions, a_i, available. This set might be finite or infinite.
- Let $a = a_1 \times \cdots \times a_n$ be the set of all profiles of pure strategies or actions, with a generic element denoted by $a = (a_1, \ldots, a_n)$.
- Player i 's payoff as a function of the vector of actions taken is

described by a function $u_i : A \to \mathbb{R}$, where $u_i(a)$ is i 's payoff if the a is the profile of actions chosen in the society.

4.2.1 Dominant Strategies

Given a game in normal form, we then can make predictions about which actions will be chosen. Predictions are particularly easy when there are dominant strategies. A dominant strategy for a player is one that produces the highest payoff of any strategy available *for every possible action by the other players.*

That is, a strategy $a_i \in a_i$ is a *dominant* (or weakly dominant) strategy for player i if $u_i(a_i, a_{-i}) \geq u_i(a_i^{'}, a_{-i})$ for all $a_i^{'}$ and all $a_{-i} \in a_{-i}$. A strategy is a strictly dominant strategy if the above inequality holds strictly for all $a_i^{'} \neq a_i$ and all $a_{-i} \in a_{-i}$.

Dominant strategies are powerful from both an analytical point of view and a players perspective. An individual does not have to make any predictions about what other players might do, and still has a well-defined best strategy.

When dominant strategies exist, they make the game-theoretic analysis relatively easy. However, such strategies do not always exist, and then we can turn to notions of equilibrium.

4.2.2 Nash Equilibrium

A pure strategy Nash equilibrium is a profile of strategies such that each players strategy is a best response (results in the highest available payoff) against the equilibrium strategies of the other players.

A strategy a_i is a *best reply*, also known as a best response, of player i to a profile of strategies $a_{-i} \in a_{-i}$ for the other players if

$$u_i(a_i, a_{-i}) \geq u_i(a_i^{'}, a_{-i}) \tag{4.1}$$

for all $a_i^{'}$. A best response of player i to a profile of strategies of the other players is said to be a *strict best response* if it is the unique best response.

A profile of strategies $a \in A$ is a *pure strategy Nash equilibrium* if a_i is a best reply to a_{-i} for each i. That is, a is a Nash equilibrium if

$$u_i(a_i, a_{-i}) \geq u_i(a_i^{'}, a_{-i}) \tag{4.2}$$

for all i and $a_i^{'}$. This definition might seem somewhat similar to that of dominant strategy, but there is a critical difference. A pure strategy Nash equilibrium only requires that the action taken by each agent be best against the actual equilibrium actions taken by the other players, and not necessarily against all possible actions of the other players.

A Nash equilibrium has the nice property that it is stable: if each player expects a to be the profile of actions played, then no player has any incentive to change his or her action. In other words, no player regrets having played the action that he or she played in a Nash equilibrium.

In some cases, the best response of a player to the actions of others is unique. A Nash equilibrium such that all players are playing actions that are unique best responses is called a *strict* Nash equilibrium. A profile of dominant strategies is a Nash equilibrium but not vice versa.

To see another illustration of Nash equilibrium, consider the following game between two firms that are deciding whether to advertise. Total available profits are 28, to be split between the two firms. Advertising costs a firm 8. Firm 1 currently has a larger market share than firm 2, so it is seeing 16 in profits while firm 2 is seeing 12 in profits. If they both advertise, then they will split the market evenly and get 14 in base profits each, but then must also pay the costs of advertising, so

they receive see net profits of 6 each. If one advertises while the other does not, then the advertiser captures three-quarters of the market (but also pays for advertising) and the non-advertiser gets one-quarter of the market. There are obvious simplifications here: just considering two levels of advertising and assuming that advertising only affects the split and not the total profitability. The net payoffs are given in Figure 4.1.

		Firm 2	
		Not	Adv
Firm 1	Not	16, 12	7, 13
	Adv	13, 7	6, 6

Figure 4.1: An Advertising Game.

To find the equilibrium, we have to look for a pair of actions such that neither firm wants to change its action given what the other firm has chosen. The search is made easier in this case, since firm 1 has a strictly dominant strategy of not advertising. Firm 2 does not have a dominant strategy; which strategy is optimal for it depends on what firm 1 does. But given the prediction that firm 1 will not advertise, firm 2 is best off advertising. This forms a Nash equilibrium, since neither firm wishes to change strategies. You can easily check that no other pairs of strategies form an equilibrium.

4.2.3 Randomization and Mixed Strategies

There are simple games for which pure strategy equilibrium do not exist. To see this, consider the 9 following simple variation on a penalty kick in a soccer match. There are two players: the player kicking the ball and the goalie. Suppose, to simplify the exposition, that we restrict the actions

to just two for each player (there are still no pure strategy equilibria in the larger game, but this simplified version makes the exposition easier). The kicking player can kick to the left side or to the right side of the goal. The goalie can move to the left side or to the right side of the goal and has to choose before seeing the kick, as otherwise there is too little time to react. To keep things simple, assume that if the player kicks to one side, then she scores for sure if the goalie goes to the other side, while the goalie is certain to save it if the goalie goes to the same side. The basic payoff structure is depicted in Figure 4.2.

		Goalie	
		L	R
Kicker	L	-1, 1	1, -1
	R	1, -1	-1, 1

Figure 4.2: A Penalty-Kick Game.

This is also the game known as matching pennies. The goalie would like to choose a strategy that matches that of the kicker, and the kicker wants to choose a strategy that mismatches the goalies strategy.

It is easy to check that no pair of pure strategies forms an equilibrium. What is the solution here? It is just what you see in practice: the kicker randomly picks left versus right, in this particular case with equal probability, and the goalie does the same. To formalize this observation we need to define randomized strategies, or what are called *mixed strategies*. For ease of exposition suppose that a_i is finite; the definition extends to infinite strategy spaces with proper definitions of probability measures over pure actions.

A *mixed strategy* for a player i is a distribution s_i on a_i, where $s_i(a_i)$ is the probability that ai is chosen. A profile of mixed strategies $(s_1, \ldots, s_n)$ forms a *mixed-strategy Nash equilibrium* if

$$\sum_a \left(\prod_j s_j(a_j) \right) u_i(a) \geqslant \sum_{a_{-i}} \left(\prod_{j \neq i} s_j(a_j) \right) u_i(a_i', a_i) \tag{4.3}$$

for all i and a_i'.

So a profile of mixed strategies is an equilibrium if no player has some strategy that would offer a better payoff than his or her mixed strategy in reply to the mixed strategies of the other players. Note that this reasoning implies that a player must be indifferent to each strategy that he or she chooses with a positive probability under his or her mixed strategy. Also, players randomizations are independent. A special case of a mixed strategy is a pure strategy, where probability 1 is placed on some action.

It is easy to check that each mixing with probability 1/2 on L and R is the unique mixed strategy of the matching pennies game above. If a player, say the goalie, places weight of more than 1/2 on L, for instance, then the kicker would have a best response of choosing R with probability 1, but then that could not be an equilibrium as the goalie would want to change his or her action, and so forth.

There is a deep and long-standing debate about how to interpret mixed strategies, and the extent to which people really randomize. Note that in the goalie and kicker game, what is important is that each player not know what the other player will do. For instance, it could be that the kicker decided before the game that if there was a penalty kick then she would kick to the left. What is important is that the kicker not be known to always kick to the left.

We can begin to see how the equilibrium changes as we change the

payoff structure. For example, suppose that the kicker is more skilled at kicking to the right side than to the left.

In particular, keep the payoffs as before, but now suppose that the kicker has an even chance of scoring when kicking right when the goalie goes right. This leads to the payoffs in Figure 4.3.

		Goalie L	Goalie R
Kicker	L	-1, 1	1, -1
	R	1, -1	0, 0

Figure 4.3: A biased penalty-kick game.

What does the equilibrium look like? To calculate the equilibrium, it is enough to find a strategy for the goalie that makes the kicker indifferent, and a strategy for the kicker that makes the goalie indifferent.

Let s_1 be the kickers mixed strategy and s_2 be the goalies mixed strategy. It must be that the kicker is indifferent. The kickers expected payoff from kicking L is $-1 \cdot s_2(L) + 1 \cdot s_2(R)$ and the payoff from R is $1 \cdot s_2(L) + 0 \cdot s_2(R)$, so that indifference requires that

$$-s2(L) + s2(R) = s2(L), \tag{4.4}$$

which implies that $2s_2(L) = s_2(R)$. Since these must sum to one (as they are probabilities), this implies that $s_2(L) = 1/3$ and $s_2(R) = 2/3$. Similar calculations based on the requirement that the goalie be indifferent lead to

$$s_1(L) - s_1(R) = -s_1(L), \tag{4.5}$$

and so the kickers equilibrium strategy must satisfy $2s_1(L) = s_2(R)$, which this implies that $s_1(L) = 1/3$ and $s_1(R) = 2/3$.

Note that as the kicker gets more skilled at kicking to the right, they both adjust to using the right strategy more. The goalie ends up using the R strategy with higher probability than before even though that strategy has gotten worse for the goalie in terms of just looking at each entry of Figure 4.3 compared to Figure 4.2. This reflects the strategic aspect of the game: each players strategy reacts to the others strategy, and not just absolute changes in payoffs as one might superficially expect. The kicker using R more means that the goalie is still indifferent with the new payoffs, and the goalie has to adjust to using R more in order to keep the kicker indifferent. While not all games have pure strategy Nash equilibrium, every game with a finite set of actions has at least one mixed strategy Nash equilibrium (with a special case of a mixed strategy equilibrium being a pure strategy equilibrium), as shown in [23].

4.3 Sequentiality, Extensive Form Games, and Backward Induction

Let us now turn to the question of timing. In the above discussion it was implicit that each player was selecting a strategy with beliefs about the other players strategies but without knowing exactly what they were. If we wish to be more explicit about timing, then we can consider what are known as games in *extensive form*, which include a complete description of who moves in what order and what they have observed when they move. There are advantages to working with extensive form games, as they allow more explicit treatments of timing and for equilibrium concepts that require credibility of strategies in response to the strategies of others.

Definitions for a general class of extensive form games are notationally intensive. Here I will just discuss a special class of extensive form gamesfinite games of perfect information which allows for a treatment that avoids much of the notation. These are games in which players move sequentially in some pre-specified order (sometimes contingent on which actions have been chosen), each player moves at most a finite number of times, and each player is completely aware of all moves that have been made previously. These games are particularly well behaved and can be represented by simple trees, where a nontermial node is associated with the move of a specified player and an edge corresponds to different actions the player might take, and terminal nodes (that have no edges following them) list the payoffs if those nodes are reached, as in Figure 4.4. I will not provide formal definitions, but simply refer directly to games representable by such finite game trees.

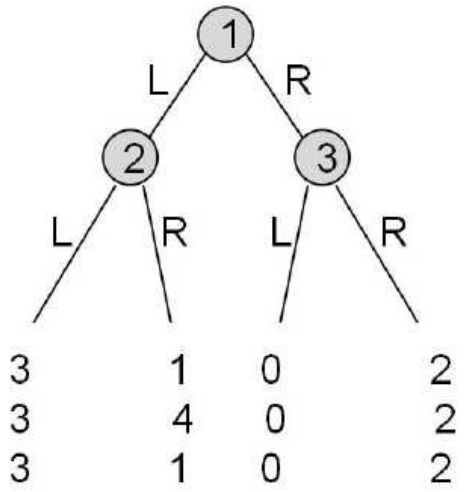

Figure 4.4: A Game Tree with 3 Players and Two Actions Each.

Each node has a players label attached to it. There is an identified *root node* that corresponds to the first player to move (player 1 in Figure

4.4) and then subsequent nodes than the two-by-two games discussed above. 14 that correspond to subsequent players who make choices. In Figure 4.4, player 1 has a choice of moving either left or right. The branches in the tree correspond to the different actions available to the player at a given node. In this game, if player 1 moves left, then player 2 moves next; while if player 1 moves right, then player 3 moves next. It is also possible to have trees in which player 1 chooses twice in a row, or no matter what choice a given player makes it is a certain player who follows, and so forth. The payoffs are given at the end nodes and are listed for the respective players. The top payoff is for player 1, the second for player 2, and the bottom for player 3. So the payoffs depend on the set of actions taken, which then determines a path through the tree. An equilibrium provides a prediction about how each player will move in each contingency and thus makes a prediction about which path will be taken; we refer to that prediction as the *equilibrium path.*

We can apply the concept of a Nash equilibrium to such games, which here is a specification of what each player would do at each node with the requirement that each players strategy be a best response to the other players strategies. Nash equilibrium does not always make sensible predictions when applied to the extensive form. For instance, reconsider the advertising example discussed above in Figure 4.1. Suppose that firm 1 makes its decision of whether to advertise before firm 2 does, and that firm 2 learns firm 1s choice before it chooses. This scenario is represented in the game tree pictured in Figure 4.5.

To apply the Nash equilibrium concept to this extensive form game, we must specify what each player does at each node. There are two Nash equilibria of this game in pure strategies. The first is where firm 1 advertises, and firm 2 does not (and firm 2s strategy conditional on firm 1 not advertising is to advertise). The other equilibrium corresponds to

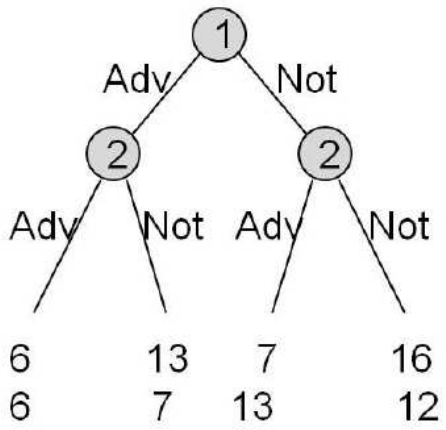

Figure 4.5: Advertising Choices of Two Competitors.

the one identified in the normal form: firm 1 does not advertise, and firm 2 advertises regardless of what firm 1 does. This is an equilibrium, since neither wants to change its behavior, given the others strategy. However, it is not really credible in the following sense: it involves firm 2 advertising even after it has seen that firm 1 has advertised, and even though this action is not in firm 2s interest in that contingency.

To capture the idea that each players strategy has to be credible, we can solve the game backward. That is, we can look at each decision node that has no successor, and start by making predictions at those nodes. Given those decisions, we can roll the game backward and decide how players will act at next-to-last decision nodes, anticipating the actions at the last decision nodes, and then iterate. This is called *backward induction*. Consider the choice of firm 2, given that firm 1 has decided not to advertise. In this case, firm 2 will choose to advertise, since 13 is larger than 12. Next, consider the choice of firm 2, given that firm 1 has decided to advertise. In this case, firm 2 will choose not to advertise, since 7 is larger than 6. Now we can collapse the tree. Firm 1 will predict

that if it does not advertise, then firm 2 will advertise, while if firm 1 advertises then firm 2 will not. Thus when making its choice, firm 1 anticipates a payoff of 7 if it chooses not to advertise and 13 if it chooses to advertise. Its optimal choice is to advertise. The backward induction prediction about the actions that will be taken is for firm 1 to advertise and firm 2 not to.

Note that this prediction differs from that in the simultaneous move game we analyzed before. Firm 1 has gained a first-mover advantage in the sequential version. Not advertising is no longer a dominant strategy for firm 1, since firm 2s decision depends on what firm 1 does. By committing to advertising, firm 1 forces firm 2 to choose not to advertise. Firm 1 is better off being able to commit to advertising in advance.

A solution concept that capture found in this game and applies to more general classes of games is known as *subgame perfect equilibrium* [24]. A subgame in terms of a finite game tree is simply the subtree that one obtains starting from some given node. Subgame perfection requires that the stated strategies constitute a Nash equilibrium in every subgame (including those with only one move left). So it requires that if we start at any node, then the strategy taken at that node must be optimal in response to the remaining specification of strategies. In the game between the two firms, it requires that firm 2 choose an optimal response in the subgame following a choice by firm 1 to advertise, and so it coincides with the backward induction solution for such a game.

It is worth noting that moving first is not always advantageous. Sometimes it allows one to commit to strategies which would otherwise be untenable, which can be advantageous; but in other cases it may be that the information that the second mover gains from knowing which strategy the first mover has chosen is a more important consideration. For example, suppose that the matching pennies game we discussed above were to

be played sequentially so that the kicker had to kick first and the goalie had time to see the kickers action and then to react and could jump left or right to match the kickers choice: the advantage would certainly then tip towards the goalie.

Chapter 5

Distribuited PA game for Noncooperative BIC-OFDM System in Smallcells Environment

In this chapter, we propose a novel Nash equilibrium (NE) problem to model concurrent communications of users who compete against each other to minimize their total allocated power (TAP) over a constraint on GP in a small cell scenario.

5.1 Introduction

Energy-efficient communications emerged as a viable design criterion for wireless communication systems in order to reduce the CO2 emission in the next years, by maximizing the amount of information (i.e. bits) that can be conveyed per Joule consumed [29]. In addition, in order to manage such a huge demand of traffic, a very promising solution is offered by

the concept of small cell (SC) networks, in which low-cost and low-power base stations, i.e. small base stations (SBSs), are massively deployed over the macro-cell areas. Their adoption allows offloading the traffic of the cellular network, increasing the offered data rate while offering at the same time a more energy-efficient architecture thanks to their reduced coverage [27]. For this reasons, in this thesis, we focus on a small cell scenario were few users are supposed to transmit over the same bandwidth. Each user wants to minimize their TAP over a constraint on QoS. Obviously, each transmitter have a limited available power, so the constraint is not also on the QoS (GP) but also in the total power allocable. We will extend the transmission model shown in Sec. 2.1 for a multiuser case. The problem is faced using the game theory. In particular, we supposed a noncooperative game, so each user try to do his best power allocation ignoring the other users. A novel iterative algorithm called *best response* (BR) is proposed to evaluate the existence of *Nash equilibrium* (NE). Simulation results are provided varying modulation, distance and constraint on GP.

5.2 System Model

5.2.1 Small cell network scenario

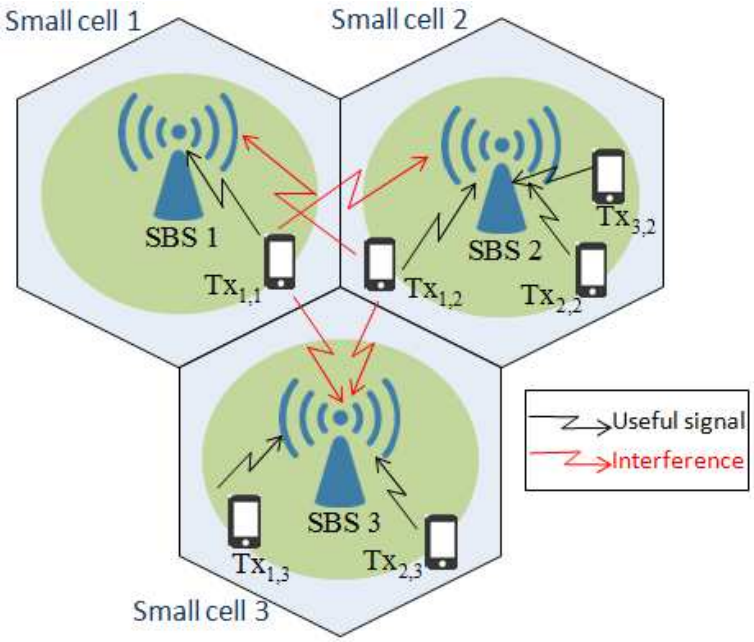

Figure 5.1: Small cell scenario with $Q = 3$ SCs.

The scenario under analysis, depicted in Fig. 5.1, is the uplink of Q small cells (SCs) belonging to the set $\mathcal{Q} \triangleq \{1, \cdots, Q\}$ and operating in OFDMA technology. Each SC exploits the same frequency band B, made of N subcarriers in the set $\mathcal{N} \triangleq \{1, \cdots, N\}$. In every SC, K_q users, in the set $\mathcal{K}_q \triangleq \{1, \cdots, K_q\}$, transmit to the relevant *small base station* (SBS) over orthogonal subbands according to the OFDMA-based access, so that intra-cell interference is avoided. Accordingly, let us denote with $\mathcal{N}_{k,q}$ the set of subcarrier assigned to user k in cell q, such that $\mathcal{N}_{k,q} \cap \mathcal{N}_{j,q} = \emptyset$ if $k \neq j$ and $\bigcup_{k \in \mathcal{K}_q} \mathcal{N}_{k,q} \subseteq \mathcal{N}$. However, they can suffer from inter-cell interference, as shown in Fig. 5.1. Interference cancelation techniques are not considered here as they would require a sizeable decoding complex-

ity and a greater quantity of signaling information among the SCs, and therefore in the following the inter-cell interference perceived at every SBS will be considered as additive colored noise.

5.2.2 BICM-OFDM Transceiver

The generic uplink between user $k \in \mathcal{K}_q$ and SBS $q \in \mathcal{Q}$ is depicted in Fig. 5.2.2. At the transmitter side, packets coming from the upper layers (usually IP packets) are processed as seen in Sec. 2.1.

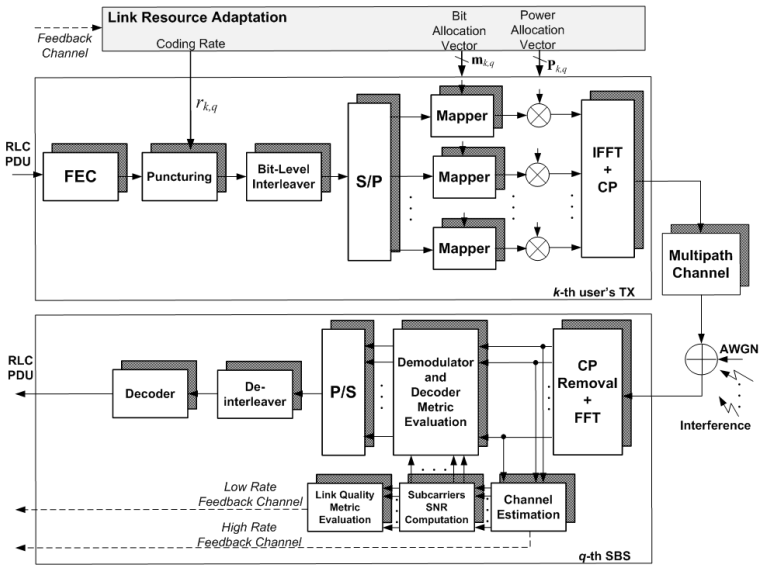

Figure 5.2: Generic BICM-OFDM link.

Extending the notation for a multi user case, at the qth SBS, the user k sample on subcarrier $n \in \mathcal{N}_{k,q}$ at the output of the DFT unit, assuming perfect channel state information, is

$$z_{k,q,n} = \sqrt{p_{k,q,n}} h_{k,q,q,n} x_{k,q,n} + t_{k,q,n} + w_{k,q,n}, \tag{5.1}$$

where

- $h_{j,s,q,n}$ denotes the channel coefficient between user j in cell s and SBS q over subcarrier n;
- $w_{k,q,n} \in \mathcal{N}(0, \sigma^2_{w_{k,q,n}})$ is the zero-mean complex-valued Gaussian random variable describing the ambient noise;
- $t_{k,q,n} \triangleq \sum_{s=1,\, s\neq q}^{Q} \sum_{j\in\mathcal{K}_s} \sqrt{p_{j,s,n}} h_{j,s,q,n} x_{j,s,n}$ is the inter-cell interference, described as additive colored Gaussian noise with zero mean and variance

$$\sigma^2_{t_{k,q,n}} \triangleq \sum_{s\neq q} \sum_{j\in\mathcal{K}_s} p_{j,s,n} |h_{j,s,q,n}|^2, \quad \forall n \in \mathcal{N}_{k,q}. \tag{5.2}$$

The post-processing SINRs vector evaluated for kth link in cell q results $\Upsilon_{k,q} \triangleq \mathbf{p}_{k,q} \odot \boldsymbol{\gamma}_{k,q}$ (the operator $\odot$ denotes the element-wise multiplication), where $\boldsymbol{\gamma}_{k,q} \triangleq [\gamma_{k,q,1}, \cdots, \gamma_{k,q,N}]^{\mathrm{T}}$, with

$$\gamma_{k,q,n} \triangleq \frac{|h_{k,q,q,n}|^2}{\sigma^2_{w_{k,q,n}} + \sum_{s\neq q} \sum_{j\in\mathcal{K}_s} p_{j,s,n} |h_{j,s,q,n}|^2} \quad \forall n \in \mathcal{N}_{k,q}, \tag{5.3}$$

0 otherwise.

5.2.3 Link Performance Model

From the knowing of the post-processing SINRs vector $\Upsilon_{k,q}$ is possible to evaluate the PER of the system. This is performed by the ESM methods seen in Sec. 2.5. As known, the ESM technique one-to-one maps the SINR vector $\Upsilon_{k,q}$ of the kth user in cell q into a single scalar value $\gamma_{k,q}$, named ESNR, representing the SNR experienced by an equivalent coded BPSK system transmitting over an AWGN channel. More precisely, the ESNR $\gamma_{k,q}$ is such that

$$PER_{r_{k,q}}(\Upsilon_{k,q}) = PER_{AWGN_{r_{k,q}}}(\gamma_{k,q}), \tag{5.4}$$

where $\mathrm{PER}_{r_{k,q}}$ and $\mathrm{PER}_{AWGN_{r_{k,q}}}$ denote the PER of the frequency-selective coded BIC-OFDM system and that of the equivalent coded binary system over AWGN channel, respectively, when both employ code rate $r_{k,q}$. The $\mathrm{PER}_{AWGN_{r_{k,q}}}$, according to [30], [31], is an analytic, monotonically decreasing, and convex function in the region of interest.

Before proceeding further, let us introduce the following useful definitions that allow to ease the notation without loss of generality. Recalling that, due to the OFDMA-based access at most one user per cell transmits over a given subcarrier, the interfence caused over the band B by the generic SC s towards the other SCs, depends on the "global" SC power and channel vectors $\mathbf{p}_s \triangleq [p_{s,1}, \cdots, p_{s,N}]^{\mathrm{T}}$ and $\mathbf{h}_{s,q} \triangleq [h_{s,q,1}, \cdots, h_{s,q,N}]^{\mathrm{T}}$ where $\mathbf{p}_s \equiv \sum_{j \in \mathcal{K}_s} \mathbf{p}_{j,s} \odot \mathbf{a}_{j,s}$ and $\mathbf{h}_{s,q} \equiv \sum_{j \in \mathcal{K}_s} \mathbf{h}_{j,s,q} \odot \mathbf{a}_{j,s}$, being $\mathbf{a}_{j,s} = [a_{j,s,1}, \cdots, a_{j,s,N}]^{\mathrm{T}}$ the subcarrier allocation vector for user j in SC s, i.e., $a_{j,s,n} = 1$ if $n \in \mathcal{N}_{j,s}$, 0 otherwise. In other words, concerning the inter-cell interference, each SC s behaves as composed by one virtual user transmitting with power $\mathbf{p}_s$ and denoted by the channel between him and the qth SC $\mathbf{h}_{s,q}$. Assuming uniform bit loading, that is, $m_{k,q,n} = m_{k,q} \in \mathcal{D}_{\mathrm{m}}$, $\forall n \in \mathcal{N}_{k,q}$, according to the κESM technique seen in Sec. 2.5.1, the ESNR $\gamma_{k,q}$ is evaluated as

$$\gamma_{k,q}(\mathbf{p}_{k,q}, \mathbf{p}_{-q}) \triangleq -\log \left(\frac{\sum\limits_{n \in \mathcal{N}_{k,q}} \sum\limits_{\mu=1}^{\sqrt{2^{m_{k,q}}}/2} \alpha_{k,q,\mu} \, \mathrm{e}^{-\frac{p_{k,q,n}}{\rho_{k,q,n,\mu}(\mathbf{p}_{-q,n})}}}{N_{k,q} m_{k,q}} \right), \qquad (5.5)$$

where $N_{k,q} = |\mathcal{N}_{k,q}|$, $\mathbf{p}_{-q} \triangleq [\mathbf{p}_1^{\mathrm{T}}, \cdots, \mathbf{p}_{q-1}^{\mathrm{T}}, \mathbf{p}_{q+1}^{\mathrm{T}}, \cdots, \mathbf{p}_Q^{\mathrm{T}}]^{\mathrm{T}}$ and $\mathbf{p}_{-q,n} \triangleq [p_{1,n}, \cdots, p_{q-1,n}, p_{q+1,n}, \cdots, p_{Q,n}]^{\mathrm{T}}$ collect the per-SC PA vectors and per-SC/per-subcarrier PA coefficients except those of SC q, respectively,

$$\rho_{k,q,n,\mu}(\mathbf{p}_{-q,n}) \triangleq \frac{\psi_{k,q,\mu}}{\gamma_{k,q,n}} = \psi_{k,q,\mu} \frac{\sigma^2_{w_{k,q,n}} + \sum_{s \neq q} p_{s,n} |h_{s,q,n}|^2}{|h_{k,q,q,n}|^2} \qquad (5.6)$$

and $\alpha_{k,q,n}$ and $\psi_{k,q,n}$ are constant values related the modulation size

adopted over the nth subcarrier by the kth user in cell q.

5.2.4 Energy efficient figure of merit

It is worth remarking that, when dealing with packet-oriented systems, users are interested in correctly receiving the entire packet, which is in fact the basic unit of information, and not only a part of it. Thus, the energy efficiency (EE) will depend on the successful transmitted rate, given by the product of the transmission rate and the packet success rate (PSR). The latter, whose expression is

$$\psi_{r_{k,q}}(\gamma_{k,q}) = 1 - PER_{AWGN_{r_{k,q}}}(\gamma_{k,q}) \tag{5.7}$$

is in fact a "global" metric that cannot be obtained as a linear expression of the successful probabilities of each subcarrier, as can be inferred from eqn. (5.4) and (5.5). In the following, we will refer to the proposed metric as GP described in (2.5.2):

$$\zeta_{k,q}(\mathbf{p}_{k,q}, \mathbf{p}_{-q}) = r_{k,q} \sum_{n \in \mathcal{N}_{k,q}} m_{k,q,n} \Psi_{r_{k,q}}(\gamma_{k,q}(\mathbf{p}_{k,q}, \mathbf{p}_{-q})). \tag{5.8}$$

The EE of the kth link in SC q will be thus evaluated in terms of goodput-to-power ratio (GPR), or

$$\eta_{k,q}(\mathbf{p}_{k,q}, \mathbf{p}_{-q}) = \frac{\zeta_{k,q}(\mathbf{p}_{k,q}, \mathbf{p}_{-q})}{\mathbf{1}^T \mathbf{p}_{k,q} + P_{k,q}^{(\mathrm{c})}}, \tag{5.9}$$

where $P_{k,q}^{(\mathrm{c})}$ denotes the cicuit power consumption.

5.2.5 Game formulation for the QoS-constraint GPR maximization problem

Assuming that there is not a centralized unit, users of different SCs must coordinate among themselves in a distributed manner in order to

reach a stable configuration. In particular, we are interested in designing a distributed power allocation algorithm so that each user maximizes its EE accounting for the interference caused by the users in the other SCs. In particular, given the reference scenario in Sec. 5.2, recalling the observations done in Sec. 3.3 and Sec. 3.4, introducing $\bar{p}_{k,q,n}$ as the maximum available power for user k in SC q and rewriting for the sake of notation $\alpha'_{k,q,n,1} + \delta\alpha'_{k,q,n,2}$ as $\alpha_{k,q,n}$ and $\bar{\mathcal{N}}_{k,q}$ as $\mathcal{N}_{k,q}$, the PA problem can be written as[1]

$$\begin{aligned} \min_{\mathbf{p}_{k,q}} \quad & u_{k,q}(\mathbf{p}_{k,q}) \\ \text{s.t.} \quad & \textstyle\sum_{n\in\mathcal{N}_{k,q}} \alpha_{k,q,n} e^{-\frac{p_{k,q,n}}{\rho_{k,q,n}(\mathbf{p}_{-q,n})}} \leq \kappa_{k,q}, \quad \text{(a)} \quad \forall k \in \mathcal{K}_q, \forall q \in \mathcal{Q}, \\ & 0 \leq p_{k,q,n} \leq \bar{p}_{k,q,n}, \qquad\qquad \text{(b)} \end{aligned} \tag{5.10}$$

where

$$u_{k,q} \triangleq \sum_{n\in\mathcal{N}_{k,q}} p_{k,q,n}. \tag{5.11}$$

We can note that (5.10.a) entails a competition for the frequency resources to be used in the uplink between every user and its relevant SBS. This problem can thus be solved by modeling it in the framework of noncooperative game theory [33], which offers an analytical framework that describes how rational entities interact and make appropriate choices so as to find their own maximum utility. Accordingly, we can introduce the game $\mathcal{G} \triangleq \{\mathcal{K}, \mathcal{P}, \mathcal{U}\}$, described as follows:

1. $\mathcal{K} \triangleq \mathcal{K}_1 \times \cdots \times \mathcal{K}_Q$ is the overall set of users (i.e., players) ;
2. $\mathcal{P} \triangleq \mathcal{P}_{1,1} \times \cdots \times \mathcal{P}_{K_Q,Q}$ is the set strategies, where the strategy of user k in SC q is its feasible PA set, defined as

$$\mathcal{P}_{k,q} \triangleq \left\{ p_{k,q,n} \mid g_{k,q}(\mathbf{p}_{k,q}, \mathbf{p}_{-q}) \leq 0, \quad 0 \leq p_{k,q,n} \leq \bar{p}_{k,q,n}, \ \forall n \in \mathcal{N}_{k,q} \right\}, \quad \forall k \in \mathcal{K}_q, \ \forall q \in \mathcal{Q}, \tag{5.12}$$

[1]In the following expression, the variable $\kappa_{k,q}$ is the same than ξ, introduced after eqn. (3.6), evaluated for user k in cell q.

with $g_{k,q}(\mathbf{p}_{k,q}, \mathbf{p}_{-q}) \triangleq \sum_{n\in\mathcal{N}_{k,q}} \alpha_{k,q,n} e^{-\frac{p_{k,q,n}}{\rho_{k,q,n}(\mathbf{p}_{-q,n})}} - \kappa_{k,q}$;

3. $\mathcal{U} \triangleq \{u_{1,1}, \cdots, u_{K_Q,Q}\}$ is the set collecting the utility functions 5.11.

In particular, the QoS constraints introduce an interdependency among the strategies of the players, i.e., $\mathcal{P}_{k,q} = \mathcal{P}_{k,q}(\mathbf{p}_{k,q}, \mathbf{p}_{-q})$. In other words the set of strategies of the generic player q depends on the other players' strategies. In this case, the solution of the game is investigated in terms of generalized Nash equilibrium (GNE), which corresponds to the case where no player can increase its payoff by changing its strategy if the others do not. Among the vectors $\mathbf{p} \in \mathcal{P}$, the vector $\mathbf{p}^* \triangleq [{\mathbf{p}^*_{1,1}}^{\mathrm{T}}, \cdots, {\mathbf{p}^*_{K_Q,Q}}^{\mathrm{T}}]^{\mathrm{T}}$ is a pure Nash Equilibrium (NE) [33] for game $\mathcal{G}$ if

$$u_{k,q}\left(\mathbf{p}^*_{k,q}\right) \leq u_{k,q}\left(\mathbf{p}'_{k,q}\right),\ \forall \mathbf{p}'_{k,q} \in \mathcal{P}_{k,q}(\mathbf{p}^*_{-q}),\ \forall k \in \mathcal{K}_q, \forall q \in \mathcal{Q}. \quad (5.13)$$

Proposition 1. If problem 5.10 is feasible, i.e. if there exist a PA vector $\mathbf{p}^{(\mathrm{f})}$, with elements $0 \leq p_{k,q,n} \leq \bar{p}_{k,q,n},\ \forall k, q, n$, such that QoS constraints (5.10.a) are met with equality, then there exists at least one PA vector $\mathbf{p}^*$ which is a GNE equilibrium of the game. Moreover, such GNE must satisfy the so-called *best response* solution in the form seen in Chap. 3 , eqn. 3.16 for each user, by solving the fixed-point system of equations

$$\mathbf{p}^*_{k,q} = \mathrm{BR}\left(\mathbf{p}^*_1, \cdots, \mathbf{p}^*_{q-1}, \mathbf{p}^*_{q+1}, \cdots, \mathbf{p}^*_Q\right), \quad \forall k, q \quad (5.14)$$

where the nth component of the best response operator is defined as

$$\left[\mathrm{BR}\left(\mathbf{p}^*_{-q}\right)\right]_n = \rho_{k,q,n}(\mathbf{p}^*_{-q}) \left[\log \Theta^*_{k,q,n} - \log \frac{\rho_{k,q,n}(\mathbf{p}^*_{-q})}{\alpha_{k,q,n}}\right]^{\bar{p}_{k,q,n}} \quad (5.15)$$

and $\Theta^*_{k,q,n}$ is such that $g_{k,q}(\mathbf{p}^*_{k,q}, \mathbf{p}^*_{-q}) = 0$.

We remark here that the fixed-point system of equations 5.14 might lead to more than one solution, especially when the channel realizations among the users are unbalanced, as usually happens in similar cases [34].

Furthermore, necessary and sufficient condition under which game 5.10 is feasible is hard to obtain and further work is required on this. In the following, we will assess this condition via simulation.

5.2.6 Players' best-response for game $\mathcal{G}$

Since we are dealing with a decentralized implementation, where no signaling among different SCs is allowed, our aim is to derive a totally distributed iterative algorithm. In fact, this allow every user to independently optimize its own PA according to the SINR perceived, which entails the interference caused by the other users. Recalling Proposition 1, a natural scheme is that based on the best response, where the only available local information $\{\gamma_{k,q,n}\}$ is fed back from SBS q to user k which can compute its PA according to 5.15, assuming other players have already played their strategies $\mathbf{p}_{-q}$. This procedure is iterated for all the users until convergence is reached, and it is summarized in Tab. 5.17, where ϵ_p denotes the required solution accuracy and N_{it} the maximum number of iterations.
Since we suppose only one user x cell, K_q=1 and k=q. So, it could be worth to introduce a lighter notation for the rest of our analysis, dropping the dependance from q (when it's possible):

- $p_{k,n}$ is the power allocated on the nth subcarrier by the kth user belonging to the kth small cell;
- $h_{k,q,n}$ denotes the channel coefficient between user k in cell k and SBS q over subcarrier n;
- $w_{k,n} \in \mathcal{N}(0, \sigma^2_{w_{k,n}})$ is the zero-mean complex-valued Gaussian random variable describing the ambient noise on the nth subcarrier experienced by the kth user belonging to the kth small cell at the kth SBS;

- N_k is the number of subcarriers assigned to user k belonging to the kth small cell.

- $\rho_{k,n}$:

$$\rho_{k,n}(\{p_{s,n}\}_{s\neq q}) \triangleq \frac{\psi_{k,n}}{\gamma_{k,n}} = \psi_{k,n}\frac{\sigma^2_{w_{k,n}} + \sum\limits_{s\neq q} p_{s,n}|h_{s,q,n}|^2}{|h_{k,k,n}|^2} \tag{5.16}$$

- κ_k is the constraint seen in eqn. (5.10.a) for the kth user in the kth SC;

- $\alpha_{k,n}$ is a constant values related the modulation size as seen in Sec. 2.5.1 , eqn. (2.17) adopted over the nth subcarrier by the kth user in cell k.

BEST RESPONSE ALGORITHM (5.17)

Iterative algorithm to solve problem (5.10) is proposed.

Input N_k, choose a feasible PA $\mathbf{p}_k^{(0)}$, $\forall q \in \mathcal{Q}$, with k=q
Initialize i=0, ϵ_p;

Do
for $q = 1, \cdots, |\mathcal{Q}|$, k=q

- **Evaluate** $\mathbf{p}_k^i$ = BR $(\mathbf{p}_{-k}^{(i-1)})$

- **Set** i=i+1;

Until
$||\mathbf{p}_k^{(i)} - \mathbf{p}_k^{(i-1)}|| \leq \epsilon_p$ for all user, for M consecutive iterations
or i=N_{it}

Output $\mathbf{p}_k^* = \mathbf{p}_k^{(i)}$ for all users

DESCRIPTION

First step - *Power vector initialization*

A simple way to initialize the power vector is to consider each user separately. We suppose for now to not consider the interference from other users. The power is initialized solving problem (3.6) seen in Chap. 3. Solution is evaluated according to eqn. (3.18).

Second step - *Iterative power allocation*

After initialize the power vectors, we start with the iterative method. As said in Sec. 5.2.5 we assume a non-cooperative game strategy. So, each user try to optimize his utility function not considering the others. The difference between the situation model seen in chapt. 3 is that now each user has to consider the inter-cell interference caused by the other transmitters. Inter-cell interference (MUI) variance for the kth user is evaluable starting from eqn. (5.2) and remembering that we suppose only one user per cell:

$$\sigma^2_{MUI_{k,n}} = \sum_{j \neq k} p_{j,n} \cdot |h_{j,q=k,n}|^2 \tag{5.18}$$

Each user has now to face not only with the ambient noise $\sigma^2_{w_{k,n}}$ but also with the MUI $\sigma^2_{k,n}$, which depends from the power allocated by the other users (except the one under analysis). We can summarize the sum of ambient noise and MUI for the generic kth user as follow:

$$\sigma^2_{n_{k,n}} = \sigma^2_{w_{k,n}} + \sigma^2_{MUI_{k,n}} \tag{5.19}$$

So, BR algorithm implement the same power allocation algorithm of the point-to-point situation. In multiuser case we have also to consider the

MUI, and this causes different *Signal to Interference plus Noise ratio* (SINR) value for each subcarrier that must be taken into account for the power allocation. In practice:

$$\sigma^2_{n_{k,n}} = \sigma^2_{w_{k,n}} + \sigma^2_{MUI_{k,n}}, \quad \text{multiuser scenario} \tag{5.20}$$
$$\sigma^2_{n_{k,n}} = \sigma^2_{w_{k,n}}, \quad \text{point-to-point scenario } (\sigma^2_{MUI_{k,n}} = 0)$$

Solution for the kth user at the ith iteration is achievable from (3.18):

$$p^{(i)}_{k,n} = \rho_{k,n}(\mathbf{p}^{(i-1)}_{-k}) \left[\log(\Theta_{k,n}) - \log \frac{\rho_{k,n}(\mathbf{p}^{(i-1)}_{-k})}{\alpha_{k,n}} \right]^+ \tag{5.21}$$
$$\text{with} \quad \Theta_{k,n} = \frac{1}{\lambda_{k,n}}$$
$$\text{and} \quad \lambda_{k,n} \quad \text{such that}$$
$$\sum_{n=1}^{N} (\alpha_{k,n} + \delta \cdot \alpha_{k,n}) \cdot e^{-\left(p^{opt}_{k,n}/\rho_{k,n}\right)} \leq \kappa_k \tag{5.22}$$

Kth user , at the ith iteration, evaluate $\sigma^2_{n_{k,n}}$, that depends on ambient noise and power allocation at the (i-1)th step from all the other user (except the kth). Then, using the point-to-point algorithm described in sect. 3.4.4, evaluate the PA for kth user. This operation is repeated for every user.

Third step - *Stop condition*

The iterative BR algorithm will stop for two distinct conditions:

1. when the power allocated in the last M iteration, for each user, belong to a fixed range of convergence. In particular:

$$p^{avg}_k - \Delta \cdot p^{avg}_k \leq \sum_{n=1}^{N} p^{(i)}_{k,n} \leq p^{avg}_k + \Delta \cdot p^{avg}_k \quad \forall\ k, \text{ for } i\text{=}i\text{-}M, \ldots, i \tag{5.23}$$

   where:

   - M is the size of the mobile window used to evaluate p^{avg}_k;

- p_k^{avg} is the average TAP evaluate as follow:

$$p_k^{avg} \triangleq \left(\sum_{i=i-M}^{i} \sum_{n=1}^{N} p_{k,n}^{(i)} \right) \Big/ M \tag{5.24}$$

- Δ indicates the width of the p_k^{avg} range. It's a value between 0 and 1.

2. when the algorithm reaches the maximum number of iteration N_{it}. When this case occurs, it means that the TAP of one or more users highly fluctuate from one iteration to another. This traduces in the fact that we never reach a situation of equilibrium. The algorithm doesn't converge and no NE is reached. In these cases, we will suppose to discard such packets before the transmission.

Final step - *Output*

Supposing the existence of a solution for problem (5.10), or rather the convergence of BR algorithm after i^* iterations, thus its solution becomes: $\mathbf{p}_k^* \triangleq \left[p_{k,1}^*, \cdots, p_{k,N}^*\right]^{\mathrm{T}}$, with

$$p_{k,n}^* = \rho_{k,n}(\mathbf{p}_{-k}^{(i-1)}) \left[\log\left(\Theta_{k,n}^*\right) - \log \frac{\rho_{k,n}(\mathbf{p}_{-k}^{(i-1)})}{\alpha_{k,n}} \right]^+ \tag{5.25}$$

$$\text{with} \quad \Theta_{k,n}^* = \frac{1}{\lambda_{k,n}^*}$$

$$\text{and} \quad \lambda_{k,n}^* \quad \text{such that}$$

$$\sum_{n=1}^{N} \left(\alpha_{k,n} + \delta \cdot \alpha_{k,n}\right) \cdot e^{-\left(p_{k,n}^{opt}/\rho_{k,n}\right)} \leq \kappa_k \tag{5.26}$$

5.3 Simulation results

We propose now some simulation's results. The objective of this simulations is to find the best modulation (in the way to minimize the TAP, as seen in Chap. 3) to adopt in a small cell environment were more than one user want to transmit under QoS constraint. The program implement a

concurrent BIC-OFDM transmission. Only one user x cell is supposed, so only inter-cell interference is considered, as said in Sec. 5.2. Simulations are proposed varying the constraint on QoS (GP x OFDM Symbol) and the number of users as shown in Fig. 5.3, 5.4, 5.5.

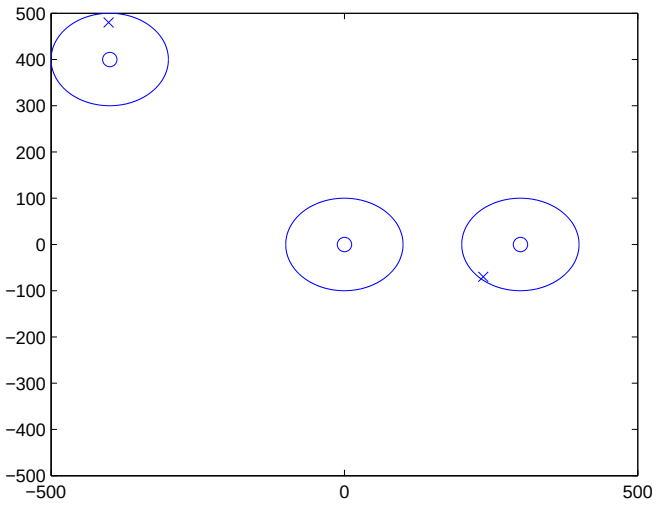

Figure 5.3: 3 cells system configuration

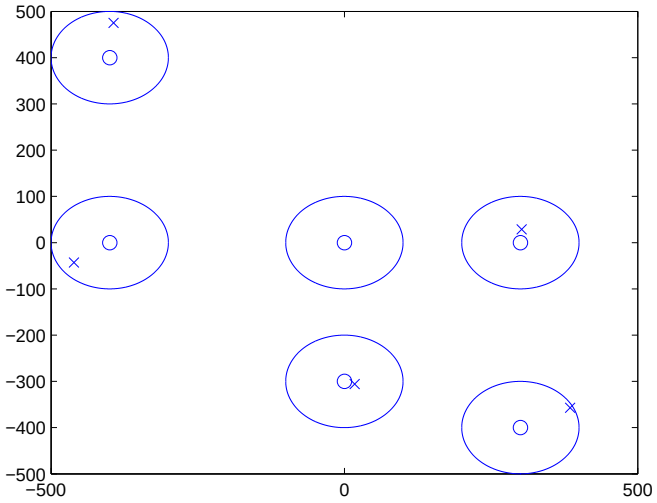

Figure 5.4: 6 cells system configuration

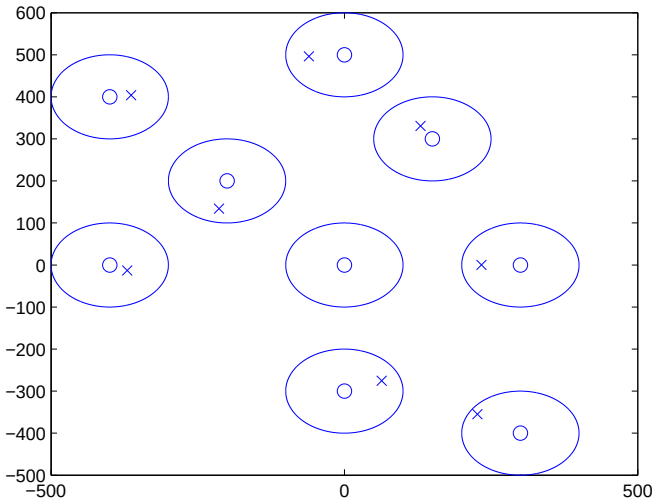

Figure 5.5: 9 cells system configuration

5.3.1 System Setup

The system used is a SISO BIC-OFDM, which has:

1. $N = 1320$ subcarriers;
2. 4-, 16- and 64-QAM as modulation format;
3. Cyclic prefix of length $N_{CP} = 160$ for the Pedestrian-B channel (see Tab. 3.2);
4. Signalling interval equal to $T = 50$ ns, corresponding to a bandwidth of $B = 20$MHz;
5. Channel encoding is based on a Turbo Encoder (TC) composed by two parallel convolutional encoder, with mother code rate r = 1/3 properly punctured to allow the eight rates 1/3, 2/5, 1/2, 4/7, 2/3, 3/4, 4/5 and 6/7;
6. Each RLC-PDU consists of $N_p = 1024$ payload binary information symbols, preceded by the CRC section of length $N_{CRC} = 32$;
7. The bitloading is uniform for every subcarrier;
8. Availabe Power = 10 dbm for every user;
9. Cell Radius = 100 m;
10. Mobile Windows width M = 10.

5.3.2 Low QoS

In this simulation, we suppose to fix the constraint on GP/OFDM Symbol = 100. The features of the simulator are:

- 10000 transmitted packets;

- Available Subcarriers = 128;
- min GP = 10;
- 3, 6, 9 active users.

Results are provided fixing the performance (GP), code rate (r) and modulation (m) for each user and varying the distance between transmitter and small base station (SBS).

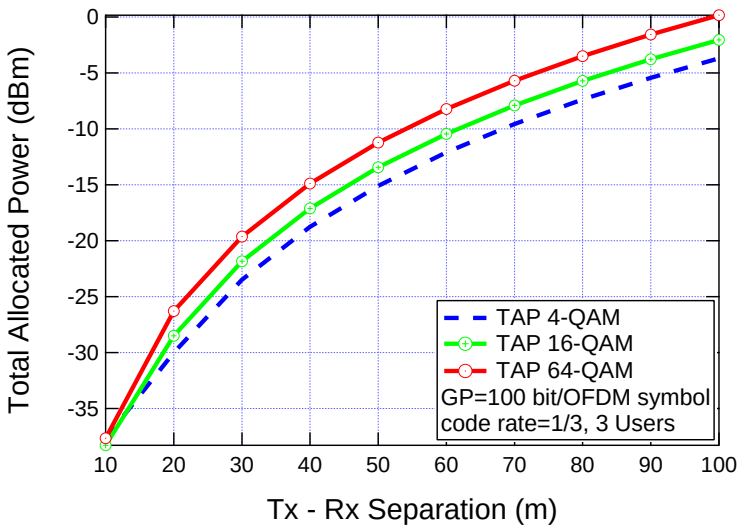

Figure 5.6: Total allocated power by 4-, 16-, 64-QAM varying the distance: GP=100 bit/OFDM-Symbol, r= 1/3, 3 users

As shown in Fig. 5.6, the modulation that minimize the TAP is the 4-QAM. To explain this behaviour can be useful to show the average number of users x link (Fig. 5.7)

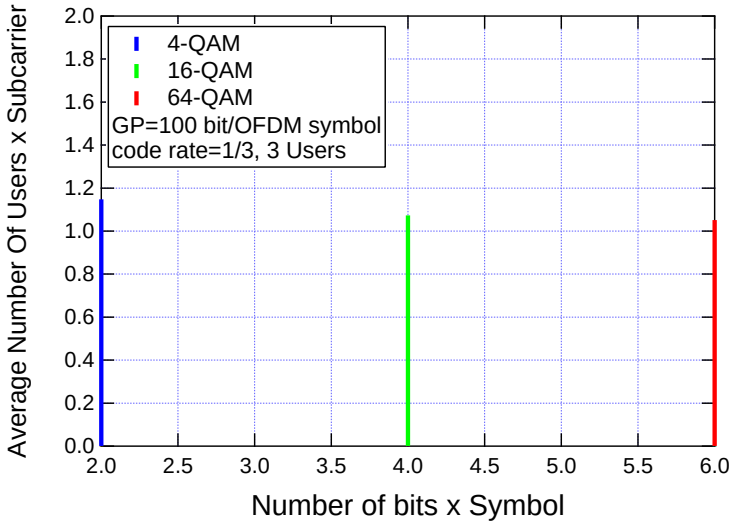

Figure 5.7: Number of users x link for 4-, 16-, 64-QAM modulation: GP=100 bit/OFDM-Symbol, r= 1/3, 3 user

The power, for each modulation, is allocated in a way to obtain a certain *estimated goodput*, evaluated before the transmission, as seen in Fig. 5.8

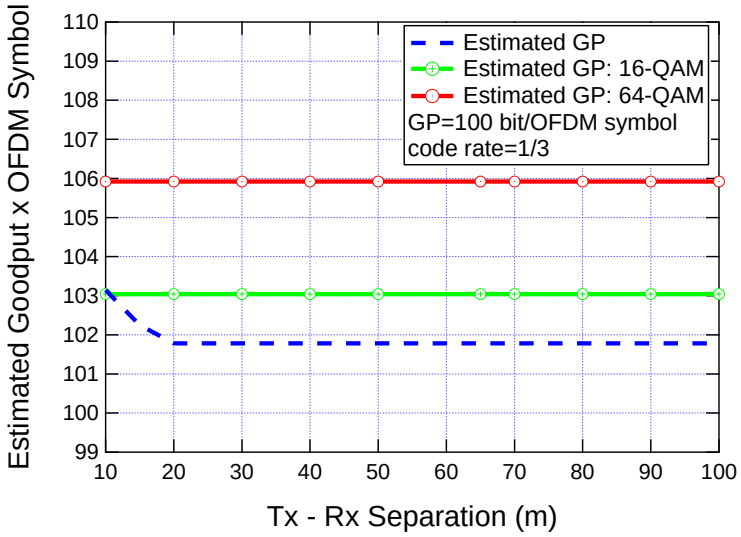

Figure 5.8: Estimated GP evaluated by 4-, 16-, 64-QAM varying the distance: GP=100 bit/OFDM-Symbol, r= 1/3

As said in Sec. 5.2.6, the BR algorithm may not converge. We supposed to discard the packets where there is not possible to find a solution at problem (3.6). In Fig. 5.38 is shown the percentage of packet's convergence for each modulation adopted. For the packets not discarded, we evaluate the speed of convergence of the algorithm in Fig. 5.9

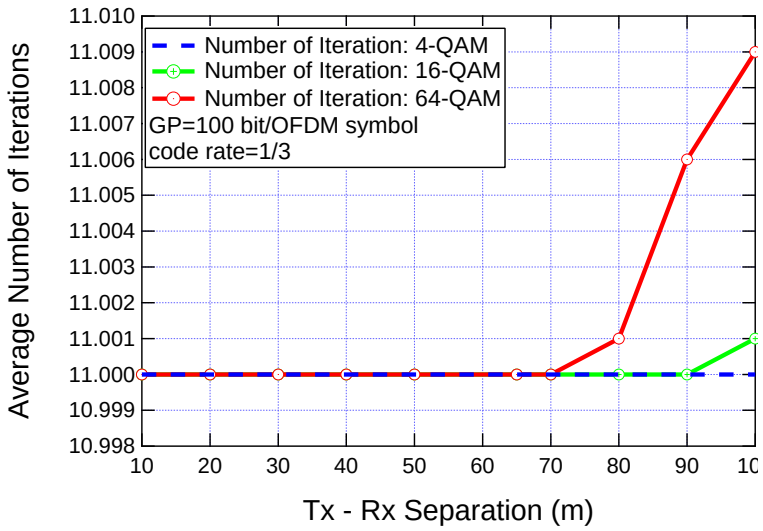

Figure 5.9: Speed of convergence of BR algorithm varying the distance: GP=100 bit/OFDM-Symbol, r= 1/3

With 6 concurrent users, simulation results are shown in Fig. 5.10, 5.11.

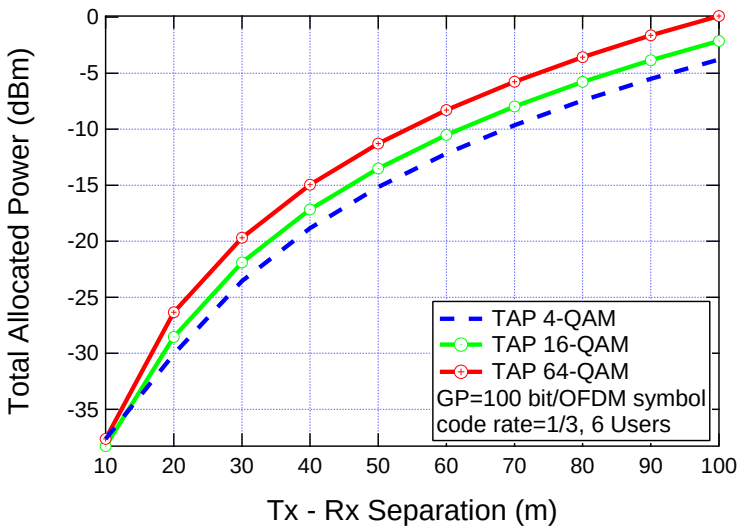

Figure 5.10: Total allocated power by 4-, 16-, 64-QAM varying the distance: GP=100 bit/OFDM-Symbol, r= 1/3, 6 user

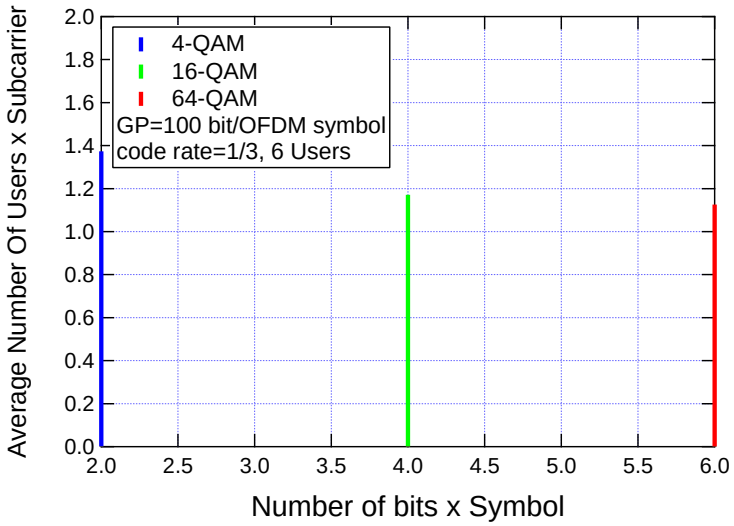

Figure 5.11: Number of users x link for 4-, 16-, 64-QAM modulation: GP=100 bit/OFDM-Symbol, r= 1/3, 6 user

In Fig. 5.12 and Fig. 5.13 we propose simulation's results for 9 concurrent users:

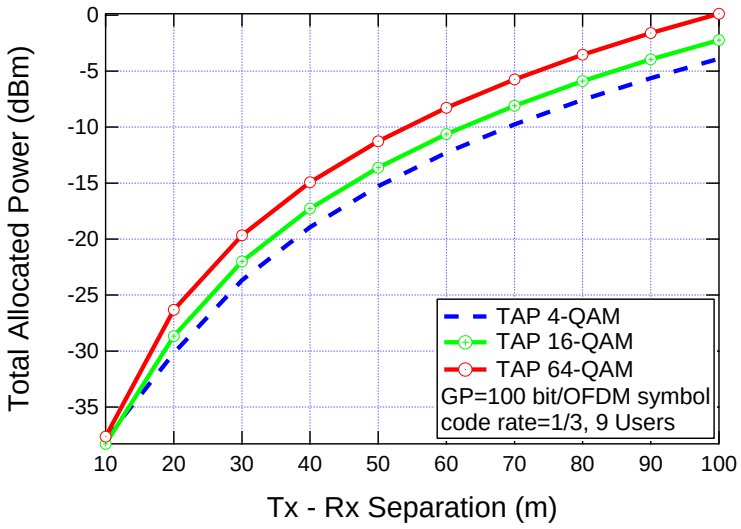

Figure 5.12: Total allocated power by 4-, 16-, 64-QAM varying the distance: GP=100 bit/OFDM-Symbol, r= 1/3, 9 user

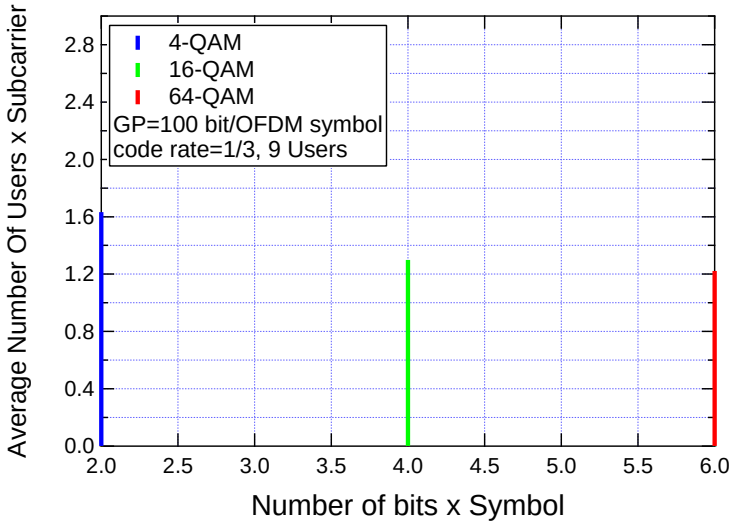

Figure 5.13: Number of users x link for 4-, 16-, 64-QAM modulation: GP=100 bit/OFDM-Symbol, r= 1/3, 9 user

As shown in Fig. 5.7, 5.11 and 5.13, each active link is used by little more than one user for each modulation. This means that the users transmit over orthogonal frequency link. The MUI is approximately 1: in practice, this situation is very similar to a point-to-point situation. As seen in Chapt. 3, in this scenario adopting a 4-QAM modulation allows to minimize the TAP, as Fig. 5.6, 5.10, 5.12 show.

5.3.3 Medium-Low QoS

In this simulation, we suppose to fix the constraint on GP/OFDM Symbol = 200. The features of the simulator are:

- 10000 transmitted packets;
- Available Subcarriers = 64;
- min GP = 10;

- 3, 6, 9 active users.

Results are provided fixing the performance (GP), code rate (r) and modulation (m) for each user and varying the distance between transmitter and small base station (SBS).

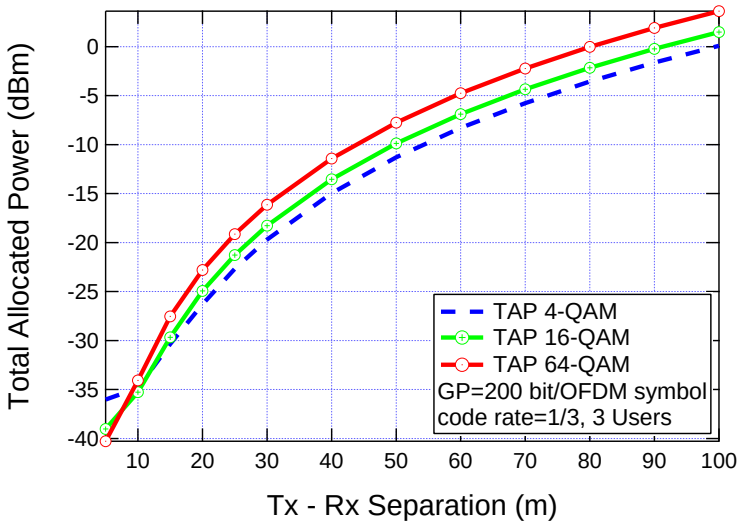

Figure 5.14: Total allocated power by 4-, 16-, 64-QAM varying the distance: GP=200 bit/OFDM-Symbol, r= 1/3, 3 user

The amount of mutual interference between the users is shown in Fig. 5.15

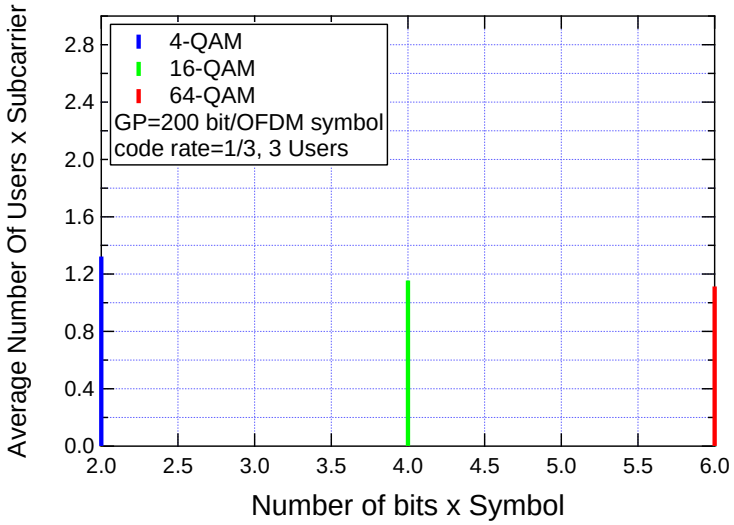

Figure 5.15: Number of users x link for 4-, 16-, 64-QAM modulation: GP=200 bit/OFDM-Symbol, r= 1/3, 3 user

The *estimated goodput* for each modulation evaluated after the BR power allocation algorithm is shown in Fig. 5.16

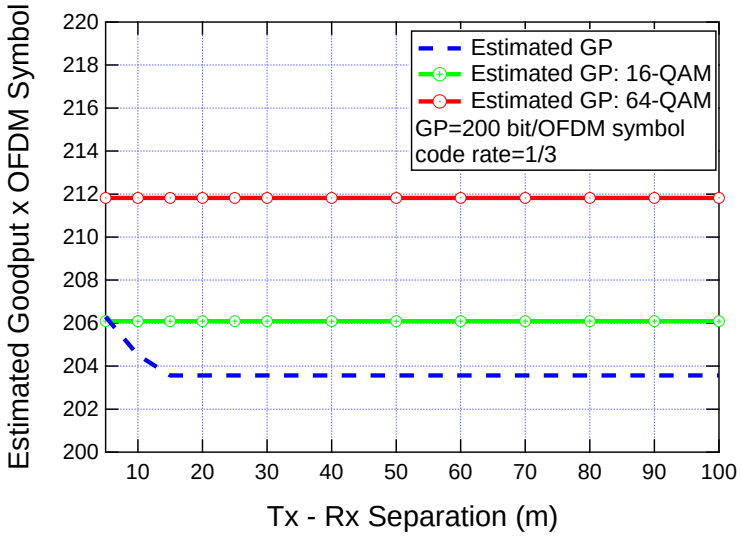

Figure 5.16: Estimated GP evaluated by 4-, 16-, 64-QAM varying the distance: GP=200 bit/OFDM-Symbol, r= 1/3

The convergence speed of the algorithm is shown in Fig. 5.17 and is independent of the number of users (3, 6 or 9).

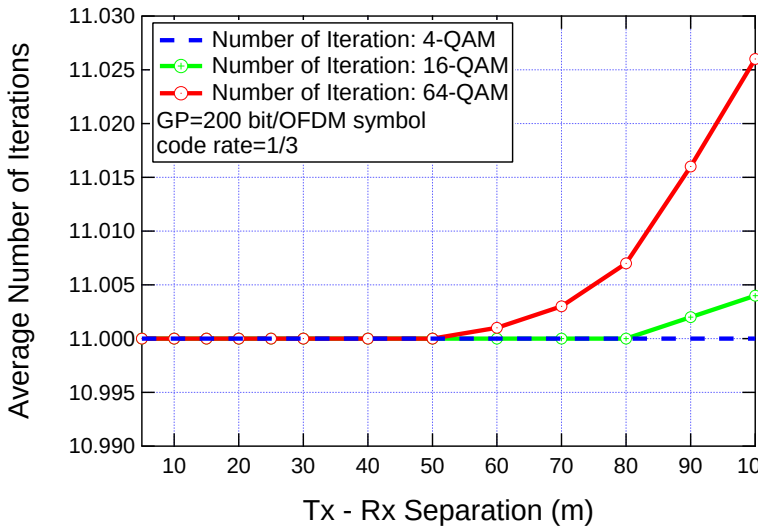

Figure 5.17: Speed of convergence of BR algorithm varying the distance: GP=200 bit/OFDM-Symbol, r= 1/3

With 6 users, results are shown in Fig. 5.18 and Fig. 5.19:

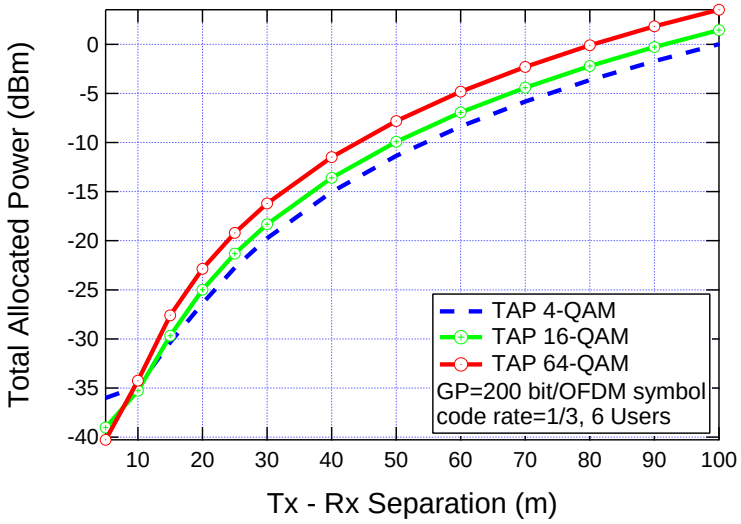

Figure 5.18: Total allocated power by 4-, 16-, 64-QAM varying the distance: GP=200 bit/OFDM-Symbol, r= 1/3, 6 user

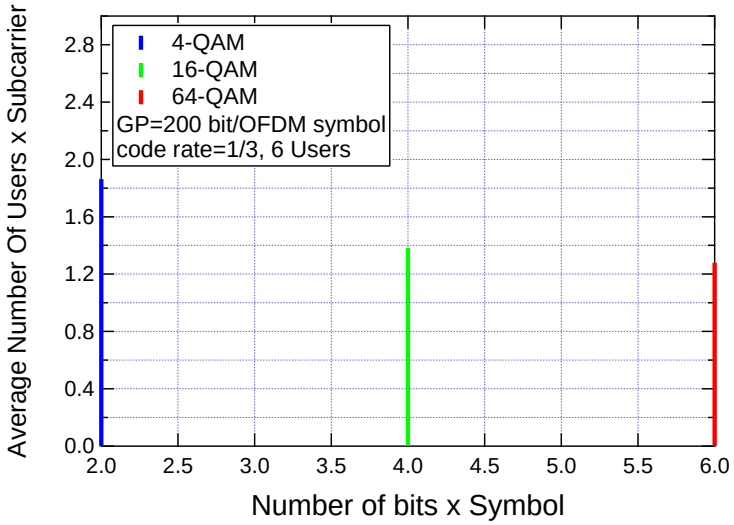

Figure 5.19: Number of users x link for 4-, 16-, 64-QAM modulation: GP=200 bit/OFDM-Symbol, r= 1/3, 6 user

Simulation's results for 9 users are proposed in Fig. 5.20 and Fig. 5.21:

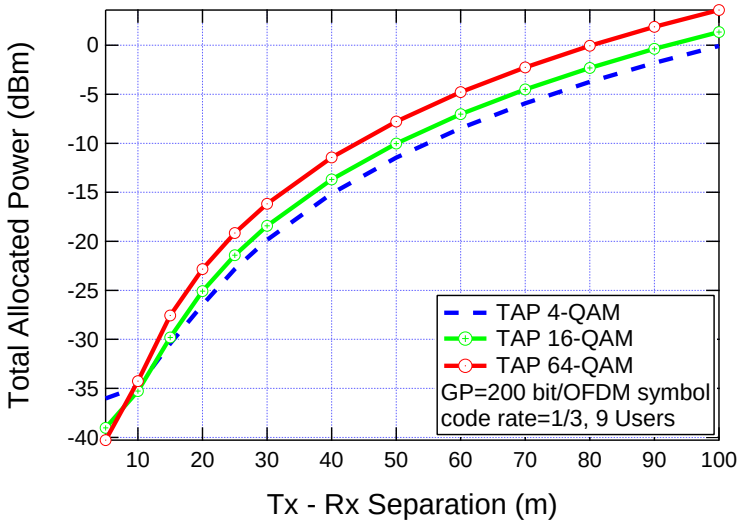

Figure 5.20: Total allocated power by 4-, 16-, 64-QAM varying the distance: GP=200 bit/OFDM-Symbol, r= 1/3, 9 user

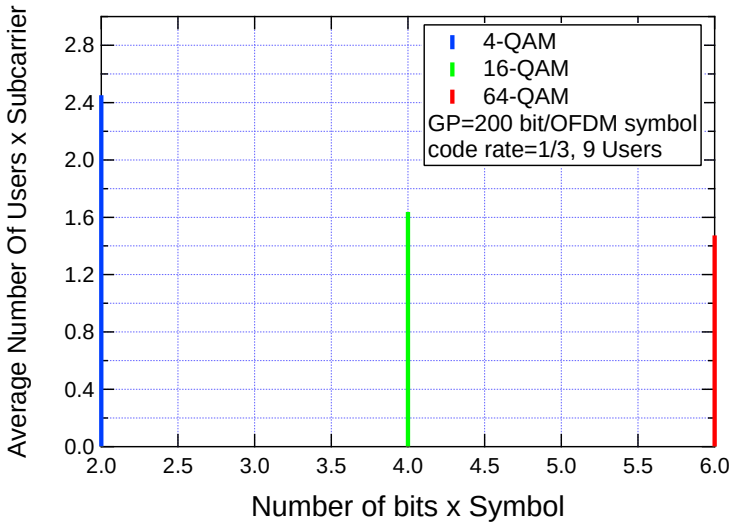

Figure 5.21: Number of user x link for 4-, 16-, 64-QAM modulation: GP=200 bit/OFDM-Symbol, r= 1/3, 9 user

As Fig. 5.14, 5.18 and 5.20 show, 4-QAM is the modulation that allocates the minimum total power. However, there is a reduced gap between the case with GP=100 (from 1.6dB to 1.4dB, as shown in Fig. 5.6, 5.10 and 5.12). In fact, growing the performance grows the number of active subcarriers needed for transmission, and so grows the MUI, as shown in Fig. 5.15, 5.19 and 5.21.

5.3.4 Medium-High QoS

In this simulation, we suppose to fix the constraint on GP/OFDM Symbol = 400. The features of the simulator are:

- 10000 transmitted packets;
- Available Subcarriers = 32;
- min GP = 10;
- 3, 6, 9 active users.

Results are provided fixing the performance (GP), code rate (r) and modulation (m) for each user and varying the distance between transmitter and small base station (SBS).

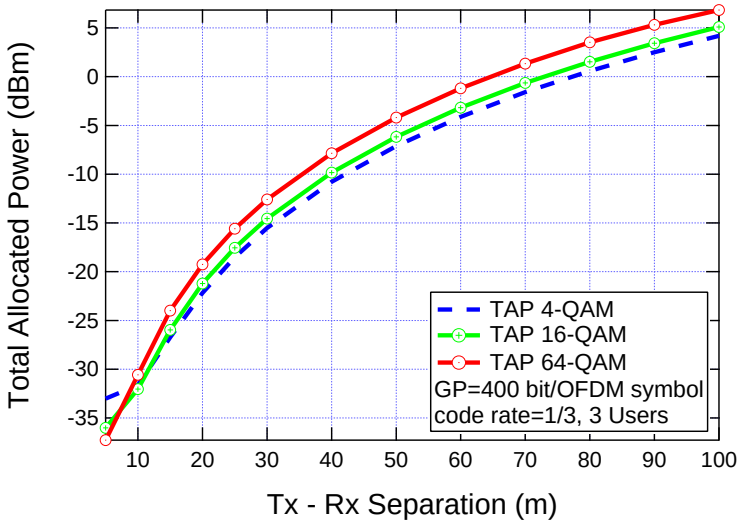

Figure 5.22: Total allocated power by 4-, 16-, 64-QAM varying the distance: GP=400 bit/OFDM-Symbol, r= 1/3, 3 user

The average number of users x link is shown in Fig. 5.23

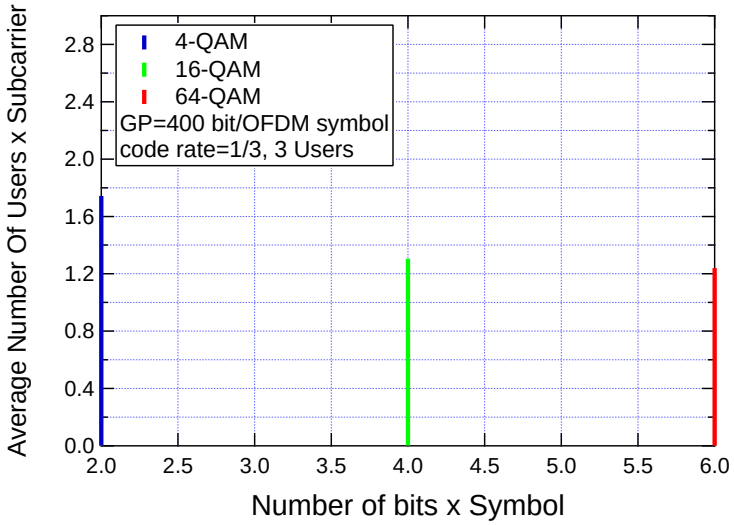

Figure 5.23: Number of users x link for 4-, 16-, 64-QAM modulation: GP=400 bit/OFDM-Symbol, r= 1/3, 3 user

The *estimated goodput* evaluated before the transmission (and independent from the number of active users) is shown in Fig. 5.24

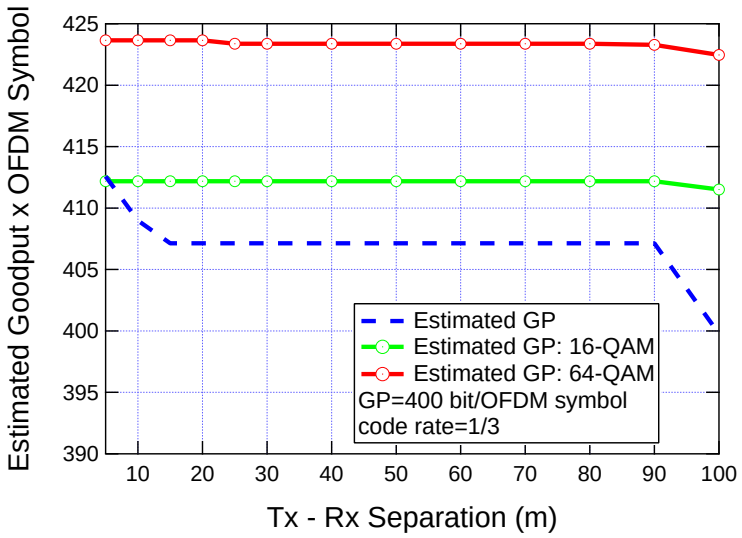

Figure 5.24: Estimated GP evaluated by 4-, 16-, 64-QAM varying the distance: GP=400 bit/OFDM-Symbol, r= 1/3

Algorithm speed is evidenced in Fig. 5.25

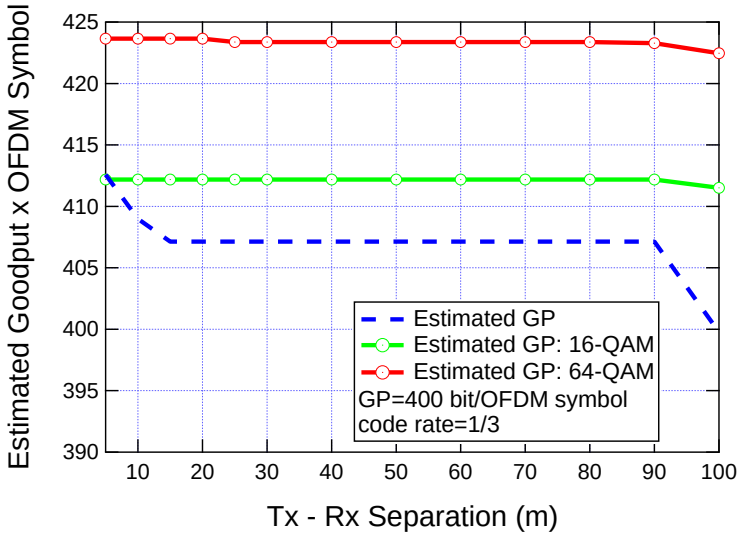

Figure 5.25: Speed of convergence of BR algorithm varying the distance: GP=400 bit/OFDM-Symbol, r= 1/3

The TAP allocated with 6 active users are shown in Fig. 5.26

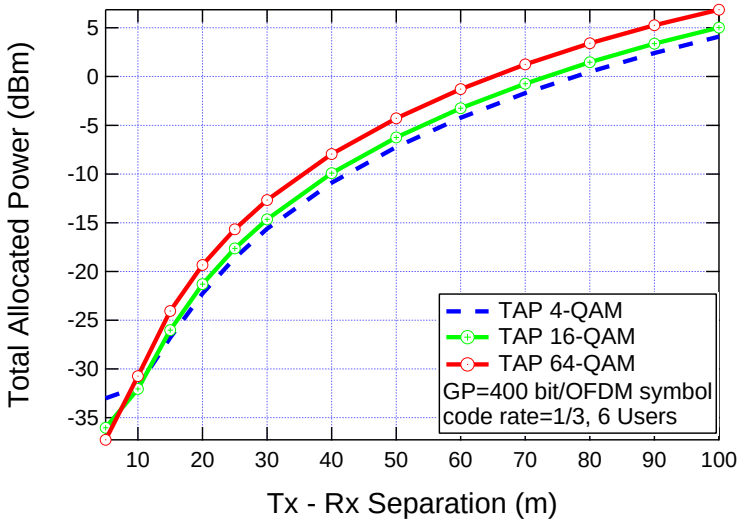

Figure 5.26: Total allocated power by 4-, 16-, 64-QAM varying the distance: GP=400 bit/OFDM-Symbol, r= 1/3, 6 user

In Fig. 5.27 is evidenced the mutual interference x active link:

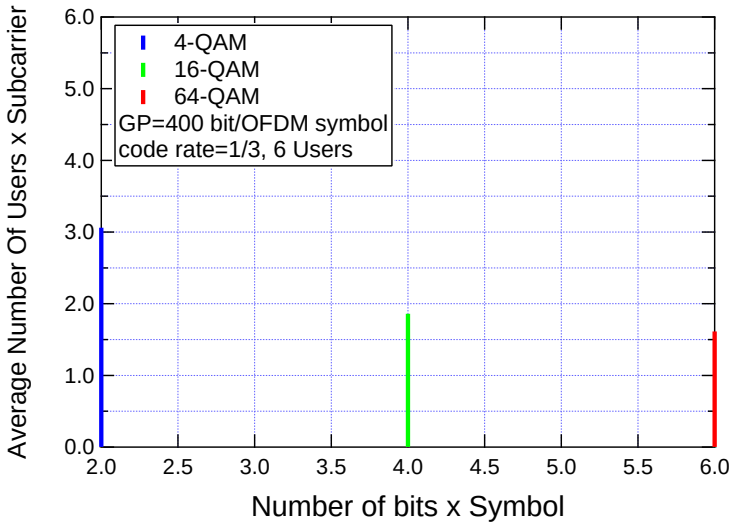

Figure 5.27: Number of users x link for 4-, 16-, 64-QAM modulation: GP=400 bit/OFDM-Symbol, r= 1/3, 6 user

Stepping to 9 users, the situation becomes the one shows in Fig. 5.28 and Fig. 5.29

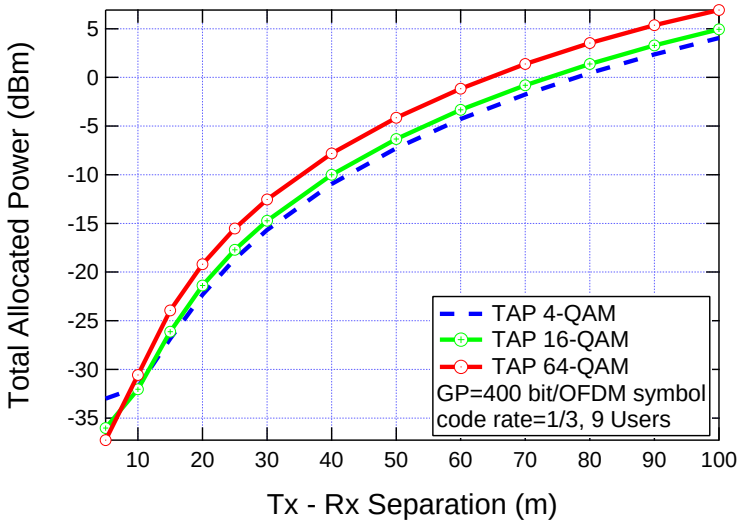

Figure 5.28: Total allocated power by 4-, 16-, 64-QAM varying the distance: GP=400 bit/OFDM-Symbol, r= 1/3, 9 user

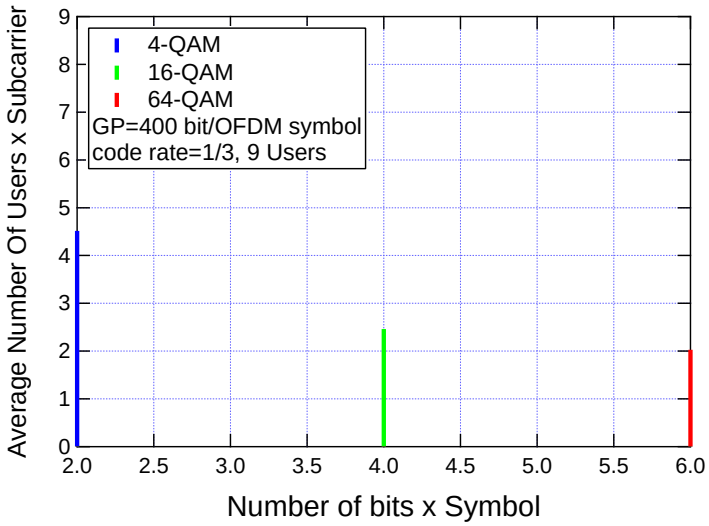

Figure 5.29: Number of users x link for 4-, 16-, 64-QAM modulation: GP=400 bit/OFDM-Symbol, r= 1/3, 9 user

As Fig. 5.23, 5.27 and 5.29, the trend described before is confirmed: to higher performances correspond higher interference x link, due to the fact that more subarriers is needed for transmissions. Then, the gap between 4- and 16-QAM is reduced (now about 1dB), as shown in Fig. 5.22, 5.26 and 5.28.

5.3.5 High QoS

In this simulation, we suppose to fix the constraint on GP/OFDM Symbol = 800. The features of the simulator are:

- 10000 transmitted packets;
- Available Subcarriers = 16;
- min GP = 10;
- 3, 6, 9 active users.

With 3 active users, results are proposed in Fig. 5.30

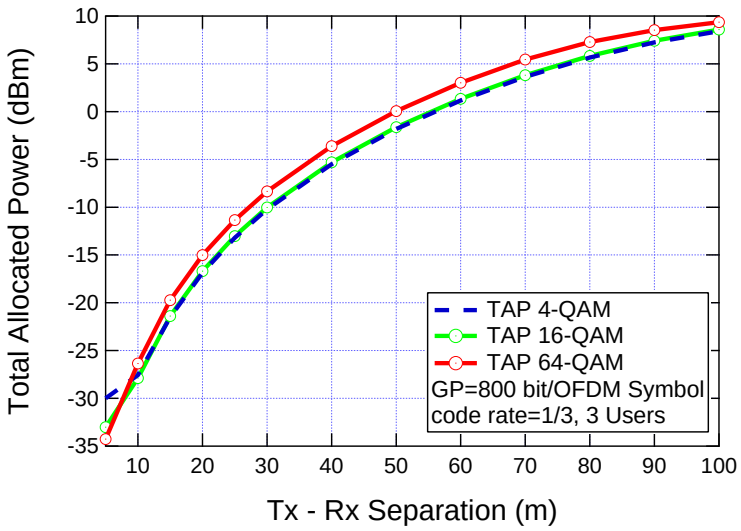

Figure 5.30: Total allocated power by 4-, 16-, 64-QAM varying the distance: GP=800 bit/OFDM-Symbol, r= 1/3, 3 user

The average interference x link is evidenced in Fig. 5.31

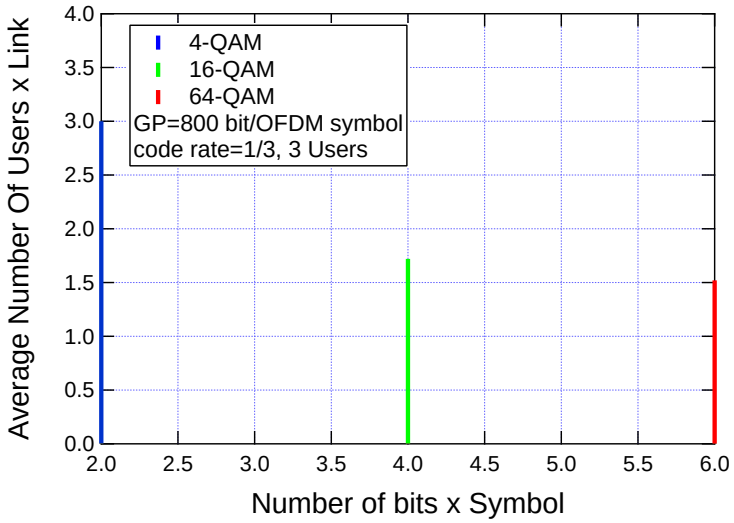

Figure 5.31: Number of users x link for 4-, 16-, 64-QAM modulation: GP=800 bit/OFDM-Symbol, r= 1/3, 3 user

The constraint on GP, evaluated before the transmission (EGP) is shown in Fig. 5.32

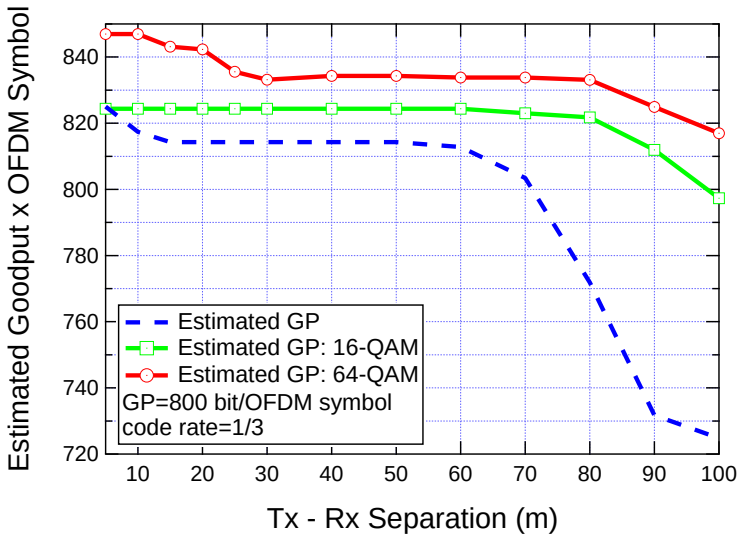

Figure 5.32: Estimated GP evaluated by 4-, 16-, 64-QAM varying the distance: GP=800 bit/OFDM-Symbol, r= 1/3

Algorithm speed is evidenced in Fig. 5.33

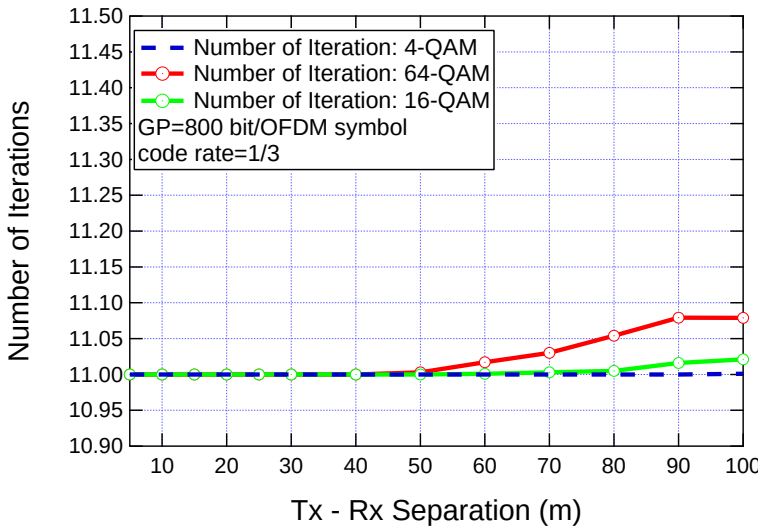

Figure 5.33: Speed of convergence of BR algorithm varying the distance: GP=800 bit/OFDM-Symbol, r= 1/3

The TAP when 6 users are transmitting is shown in Fig. 5.34

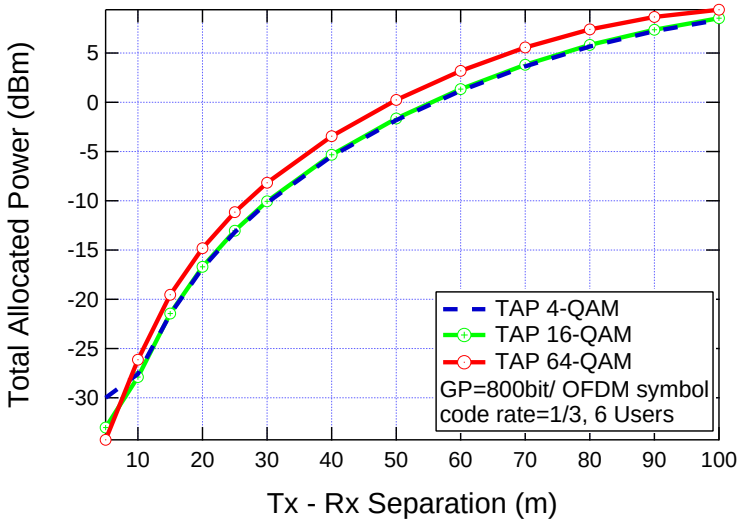

Figure 5.34: Total allocated power by 4-, 16-, 64-QAM varying the distance: GP=800 bit/OFDM-Symbol, r= 1/3, 6 user

The average interference x link is evidenced in Fig. 5.35

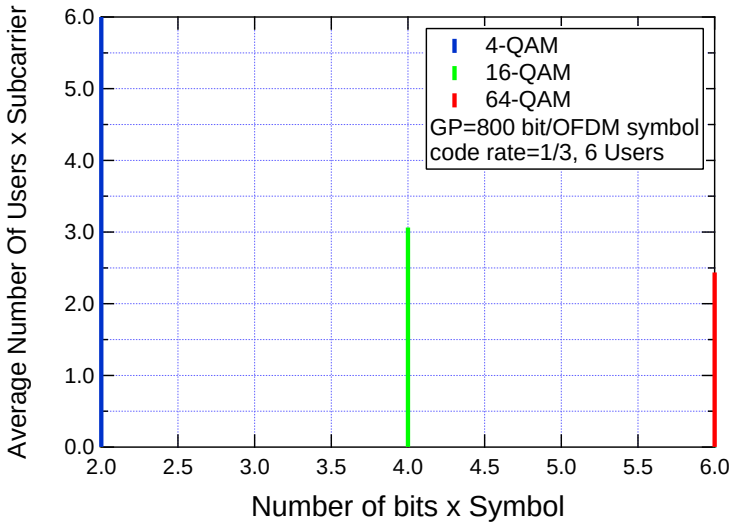

Figure 5.35: Number of users x link for 4-, 16-, 64-QAM modulation: GP=800 bit/OFDM-Symbol, r= 1/3, 6 user

Increasing the number of users to 9, results for TAP and MUI are shown in Fig. 5.36 and Fig. 5.37.

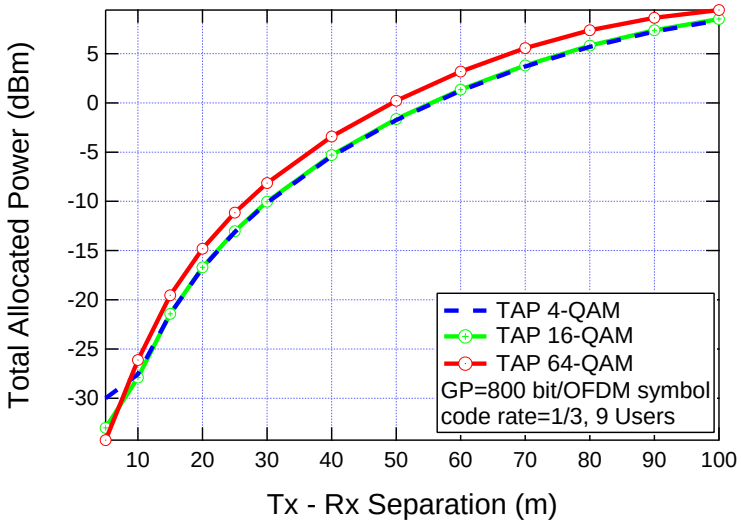

Figure 5.36: Total allocated power by 4-, 16-, 64-QAM varying the distance: GP=800 bit/OFDM-Symbol, r= 1/3, 9 user

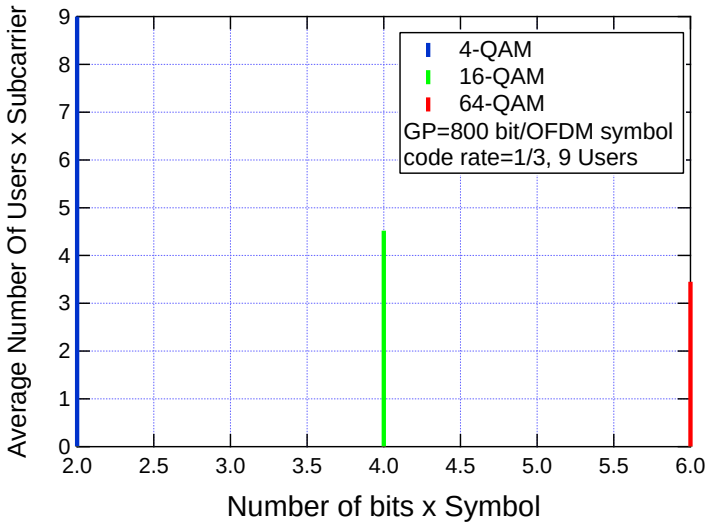

Figure 5.37: Number of users x link for 4-, 16-, 64-QAM modulation: GP=800 bit/OFDM-Symbol, r= 1/3, 9 user

As Fig. 5.30, 5.34 5.36 show, in case of high MUI, the performance of 4-QAM and 16-QAM tends are practically superimposed. This behaviour can be explained looking at Fig. 5.31, 5.35, 5.37. In these figures, we can see an high MUI, specially in 4-QAM modulation. When this modulation is adopted, the amount of MUI is equal to the number of active user. That means that all users use all the available subcarriers, and it's traduces in a high mutual interference. This situation is partially avoided by using grower modulation that need a less number of subcarriers for the transmission.

In conclusion, in Fig. 5.38 is shown the percentage of convergence of best response algorithm. The results is provided for high QoS and 9 users, that is the most stressed situation that we have analyzed.

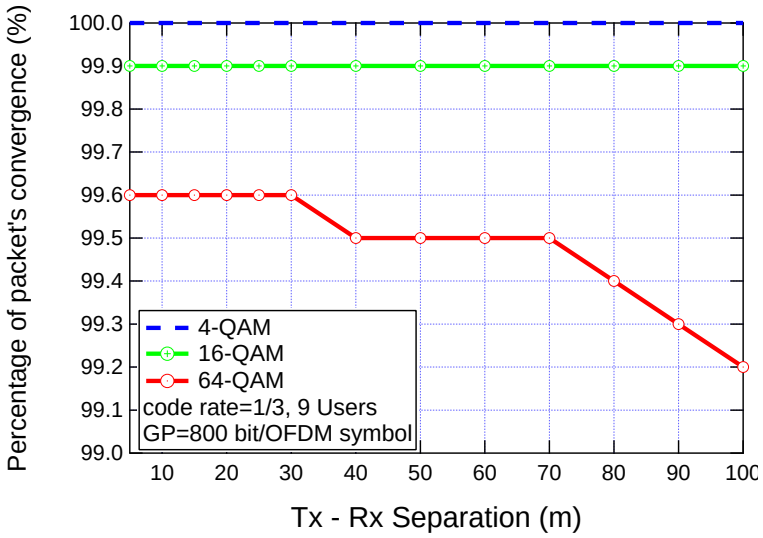

Figure 5.38: Percentage of packet's convergenze vs Distance: GP=800 bit/OFDM-Symbol, r= 1/3, 9 user

As Fig. 5.38 shows, the algorithm has an high percentage of convergence for any modulation. In particular, for 4- and 16-QAM, the percentage of convergence is about 99.9.

Chapter 6

Conclusion

In this thesis, we focused on a noncooperative scenario wherein primary users and secondary devices based on packet-oriented BIC-OFDM try to minimize their TAP over a constraint on QoS, for energy-efficient communications. We first have analyzed a point-to-point scenario and introduced a new method to estimate the power allocated over each subcarrier by the primary user. Then, we step to a small-cell multiuser scenario, where 3, 6 or 9 user try to transmit concurrently over the same spectral resource. Small-cell scenario was introduced as a novel solution of the problem of shortage of capacity in radio communication system. For short, our problem was to minimize the TAP for each user, belonging to different small cells, over a constraint on QoS. This problem was managed with the help of Game Theory. In particular, we resorted to noncooperative games, where the stable output, i.e., the Nash equilibrium, represents a feasible set of power allocation vectors that minimizes the TAP of each user. Simulation results are proposed, varying the number of users and QoS constraint. Results show that:

- GP/OFDM Symbol = 100.
  In this cases, as Fig. 5.7, 5.11 and 5.13 show, the average number

of users x link is about 1. As said, these kind of scenario is very similar to a point-to-point situation, were a 4-QAM modulation should be adopted to minimize the TAP, as Fig. 5.6, 5.10 and 5.12 show.

- GP/OFDM Symbol = 200.
  The increase of the performance requires more active subcarriers for each user, and it traduces in a higher value of users x link respect to the previous case, as Fig. 5.15, 5.19 and 5.21 show. Anyway, 4-QAM is still the best modulation in the way to minimize the TAP for each user as Fig. 5.14, 5.20 and 5.20 show , although the gap between 4-QAM and 16-QAM is smaller than the previous case (about 1.4dB respect the previous case where the gap was about 1.6dB)

- GP/OFDM Symbol = 400.
  In these cases, the GAP between 4-QAM and 16-QAM is very low (about 1dB), as Fig. 5.22, 5.26 and 5.28 show. This is due to the fact that the average number of users x link is significantly increased, as Fig. 5.23, 5.27 and 5.29 show. In this kind of situation, were the QoS required is high, or the available bandwidth is small, it could be worth to use a 16-QAM modulation. In fact, though the 4-QAM use a bit less of power, it could be difficult, especially for high distance (>80m) reach the constraint on QoS as Fig. 5.24. In fact, if not all the users reach the QoS constraint, there is an outage situation.

- GP/OFDM Symbol =800.
  In this case, as Fig. 5.30, 5.34 and 5.36 show, performance of 4-QAM and 16-QAM is superimposed. Adopting a 16-QAM guarantees a less interference x link, as Fig. 5.31, 5.35 and 5.37 show.

Beyond that, the constraint on QoS is better satisfied by 16-QAM than 4-QAM as Fig. 5.32 shows.

Concluding, results show how, in a small cell environment , 4-QAM is the modulation that minimize the TAP in situation where performances are not extremely high or the available bandwidth guarantees a low MUI. Vice versa, in situation were is required an high QoS or the available bandwidth for the transmission generate an high MUI, 16-QAM is the best modulation in the way to minimize the TAP. In fact, even if the TAP for 4- and 16-QAM is about the same, as Fig. 6.1 shows, using a 4-QAM when high QoS is required may cause an outage situation. In fact, due to the high MUI experienced, some users can not reach the constraint on QoS.

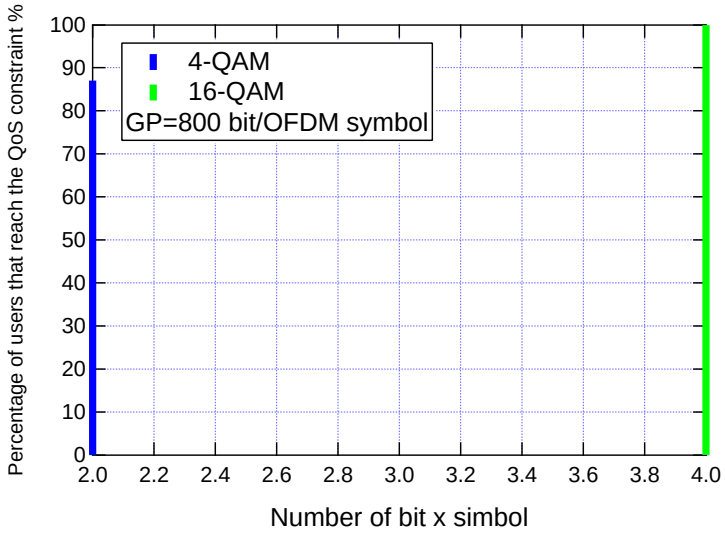

Figure 6.1: Percentage of users that reach the constraint on QoS: GP=800 bit/OFDM-Symbol, r= 1/3

Growing the number of users has the only effect to increase the mutual interference x link, reducing the gap between 16-QAM and 4-QAM.

Results are independent from distance, except in high interference cases were 4-QAM not always reaches the constraint on QoS (unlike 16- and 64-QAM). Results show also that is not worth to adopt a 64-QAM modulation, except for very low distances (>10 m), where however the TAP is very low because of the proximity between transmitter and SBS.

Bibliography

[1] P. Ciacci, "Bit loading for next generation wireless OFDM systems: a "greedy" approach for goodput optimization", *University of Pisa, Department of Information Engineering, Masters Thesis in Telecommunication Engineering*, 20 July 2009.

[2] M.-O. Pun, M. Morelli, and C.-C. J. Kuo, Multi-Carrier Techniques for Broadband Wireless Communications. A Signal Processing Perspective. Imperial College Press, London, UK, 2007

[3] J. G. Proakis, Digital Communications, 4th ed. New York, NY: McGraw- Hill, 2001.

[4] 3GPP, Technical specification group radio access network, TR 25.890 V1.0.0.

[5] K. Brueninghaus, D. Astely, T. Salzer, S. Visuri, A. Alexiou, S. Karger, and G.-A. Seraji, Link performance models for system level simulations of broadband radio access systems, in IEEE 16th International Symposium on Personal, Indoor and Mobile Radio Communications, 2005. PIMRC 2005., vol. 4, Sept. 2005, pp. 2306 2311 Vol. 4.

[6] Y. Blankenship, P. Sartori, B. Classon, V. Desai, and K. Baum, Link error prediction methods for multicarrier systems, in IEEE 60th Ve-

hicular Technology Conference, 2004. VTC2004-Fall., vol. 6, Sept. 2004, pp. 4175 4179.

[7] WINNER, Assessment of advanced beamforming and MIMO technologies, Information society technologies, D2.7, ver1.0. Standardization Document, EU project, 2003.

[8] E. Tuomaala and H. Wang, Effective SINR approach of link to system mapping in OFDM/multi-carrier mobile network, in 2nd International Conference on Mobile Technology, Applications and Systems, 2005, Nov. 2005, pp. 15.

[9] R. Srinivasan et al, Project 802.16m evaluation methodology document (EMD), IEEE 802.16m-08/004r5, Tech. Rep., Jan. 2009.

[10] S. Tsai, Effective-SNR mapping for modeling frame error rates in multiple-state channels, 3GPP2-C30-20030429-010, April 2003.

[11] W. Hai, W. Lei, and L. Min, HSDPA link adaptation based on novel quality model, in 2005 IEEE 61st Vehicular Technology Conference, 2005. VTC 2005-Spring., vol. 1, May-June 2005, pp. 334 338 Vol. 1.

[12] I. Stupia, V. Lottici, F. Giannetti, and L. Vandendorpe, Link resource adaptation for multiantenna bit-interleaved coded multicarrier systems, IEEE Transactions on Signal Processing, vol. 60, no. 7, pp. 3644 3656, July 2012.

[13] A. Guillen i Fabregas, A. Martinez, and G. Caire, Bit-interleaved coded modulation, Foundations and Trends in Communications and Information Theory, 2008.

[14] S. Cui, A. J. Goldsmith and A. Bahai, Energy-Constrained Modulation Optimization, IEEE Transactions on Wireless Communications, vol. 4, No. 5, pp. 2349-2360, 2005.

[15] G. Miao, N. Himayat, G. Y. Li and D. Bormann, Energy-Efficient Design in Wireless OFDMA, in Proc. IEEE ICC 2008, 2008.

[16] Stephen P. Boyd, Lieven Vandenberghe, "Convex Optimization", 2004

[17] Bertrand Devillers, Jrme Louveaux, and Luc Vandendorpe, "Bit and Power Allocation for Goodput Optimization in Coded Parallel Subchannels With ARQ", IEEE 2008

[18] Smart 2020: Enabling the low carbon economy in the information age, The Climate Group and Global e-Sustainability Initiative (GeSI), Tech. Rep., 2008. Available: http://www.smart2020.org

[19] Y. Chen, S. Zhang, S. Xu, and G. Li, Fundamental trade-offs on green wireless networks, IEEE Commun. Mag., vol. 49, no. 6, pp. 3037, Jun. 2011.

[20] Greentouch 2012-2013 annual report, Green Touch Consortium, Tech. Rep., 2013. Available: http://www.greentouch.org

[21] M. O. Jackson, "A Brief Introduction to the Basics of Game Theory", *Stanford University.*

[22] J. von Neumann and O. Morgenstern, "Theory of Games and Economic Behavior".

[23] J. Nash, "Non-Cooperative Games", *Annals of Mathematics 54:286 - 295,1951.*

[24] R. Selten "Reexamination of the Perfectness Concept for Equilibrium Points in Extensive Games", International Journal of Game Theory 4:25 - 55,1975

[25] G. Caire, G. Taricco, and E. Biglieri, "Bit-Interleaved Coded Modulation," *IEEE Trans. on Inf. Theory*, vol. 44, no. 5, pp. 927–946, May 1998.

[26] A. Goldsmith, and S.-G. Chua, "Variable-rate variable-power MQAM for fading channels," *IEEE Trans. on Commun.*, vol. 45, no. 10, pp. 1218 1230, Oct. 1997.

[27] J. Hoydis, M. Kobayashi, and M. Debbah, "Green small-cell networks," *IEEE Veh. Technol. Mag.*, 2011.

[28] The Climate Group and Global e-Sustainability Initiative (GeSI), 2008. SMART 2020: Enabling the low carbon economy in the information age. Available online at `http://www.smart2020.org/`.

[29] E.V. Belmega and S. Lasaulce, "Energy-efficient precoding for multiple-antenna terminals," *IEEE Trans. on Signal Proc.*, vol. 59, no. 1, pp. 329340, 2011.

[30] L. Song, and N. B. Mandayam, "Hierarchical SIR and Rate Control on the Forward Link for CDMA Data Users Under Delay and Error Constraints," *IEEE J. on Sel. Areas Commun.*, vol. 19, no. 10, pp. 1871–1882, Oct. 2001.

[31] H. Seo, and B. G. Lee, "Optimal Transmission Power for Single- and Multi-Hop Links in Wireless Packet Networks with ARQ Capability," *IEEE Trans. on Commun.*, vol. 55, no. 5, pp. 996–1006, May 2007.

[32] G. Miao, N. Himayat, G. Y. Li, and S. Talwar, "Distributed interference-aware energy-efficient power optimization," *IEEE Trans. on Wireless Commun.*, vol. 10, pp. 13231333, April 2011.

[33] M.J. Osborne, A. Rubinstein, "A Course in Game Theory", The MIT Press, 1994.

[34] J.-S. Pang, G. Scutari, F. Facchinei, and C. Wang, "Distributed power allocation with rate constraints in Gaussian Parallel Interference Channel," *IEEE Trans. on Inf. Theory*, Vol. 54, No. 8, Aug. 2008.

[35] I. Stupia, F. Giannetti, V. Lottici, R. Andreotti, L. Vandendorpe L., N. A. DAndrea, "A Greedy Algorithm for Goodput-Oriented AMC in Turbo-Coded OFDM," *in Proc. of FUNEMS 2010*, Florence, Italy.

Ringraziamenti

Vorrei iniziare ringraziando sentitamente il Prof. Giannetti e l'Ing. Lottici per avermi permesso di realizzare questo lavoro.
Un grazie particolare all'Ing. Riccardo Andreotti che mi stato di grande supporto e aiuto in questi mesi, guida indispensabile per la stesura di questa tesi.

Enorme ringraziamento anche a tutto lo staff del laboratorio A-104, in particolare a Leo e Paolo che mi hanno sempre accolto con gentilezza e aiutato con la loro disponibilita', oltre che strappato un sorriso durante la giornata.

Un grande grazie a tutta la mia famiglia, senza il loro sacrificio e supporto anche nei momenti difficili non sarei mai arrivato dove sono adesso.

Grazie a Picchia, Mazzo, Massino, Luca Doc, Emy, Ciccio, Adri che mi hanno sostenuto con la loro presenza e i loro sorrisi in tutti questi anni. Amici veri.

Un grazie ad Ale che si e' trovata a dover sopportare i miei umori in questi mesi di tesi, spero ne sia valsa la pena.

Infine grazie anche a te Toby, che c'hai sempre creduto.